



<http://dx.doi.org/10.11646/zootaxa.4007.2.1>

<http://zoobank.org/urn:lsid:zoobank.org:pub:BE8908FC-362C-4904-BB73-7E24B8169AB5>

Morphological and genetic variation in North Atlantic giant file clams, *Acesta* spp. (Bivalvia: Limidae), with description of a new cryptic species in the north-west Atlantic

JEAN-MARC GAGNON¹, ELLEN KENCHINGTON², ANTONY PORT³, LYNNE J. ANSTEY² & FRANCISCO JAVIER MURILLO²

¹Canadian Museum of Nature, P.O. Box 3443, Station D, Ottawa, ON, Canada K1P 6P4. E-mail: jmgagnon@mus-nature.ca

²Ocean and Ecosystem Sciences Division, Fisheries and Oceans Canada, Bedford Institute of Oceanography, P.O. Box 1006, 1 Challenger Dr., Dartmouth, NS, Canada B2Y 4A2. E-mail: ellen.kenchington@dfo-mpo.gc.ca

³436 Galatina Way, Ottawa, ON, Canada K2K 0E5. E-mail: portantony@gmail.com

Abstract

We analyze the morphological and genetic variability within and between seven species of *Acesta* and specimens recently collected in the northwest Atlantic using traditional morphological measurements, landmark-based geometric morphometrics, and the cytochrome oxidase subunit I (COI) gene sequences, with particular emphasis on North Atlantic species. Shell morphology and external shell appearance do not allow reliable distinction between the widely recognized northeastern Atlantic *A. excavata* and other northwest Atlantic species or populations of *Acesta*, with the exception of *A. oophaga*. Similarly, shape analysis reveals a wide variability within northeastern Atlantic *A. excavata*, and significant morphological overlap with *A. bullisi* from the Gulf of Mexico and *A. rathbuni* from the southwestern Pacific and South China Sea. Specimens from the northwestern and Mid-Atlantic display shell shapes marginally similar to that of *A. excavata*. These differences are at least partly related to anterior or posterior shifting of the shell body and to the opposite shifting of the hinge line/dorsal region and upper lunule. These morphological variations, along with the midline-width-ratio, explain much of the variability extracted by principal component analysis. Results from a mitochondrial DNA barcode approach (COI), however, suggest that the northwest Atlantic specimens belong to a new species for which we propose the name *Acesta cryptadelphe* sp. nov. Differences in larval shell sizes between northeastern and northwestern Atlantic specimens are consistent with this result.

Key words: Newfoundland, Nova Scotia, deep-water canyons, geometric morphometrics, shape analysis, COI

Résumé

Nous analysons la variabilité morphologique et génétique intra- et interspécifique de sept espèces d'*Acesta* et de spécimens récemment collectés dans le nord-ouest de l'Atlantique en utilisant des mesures morphologiques traditionnelles, la morphométrie géométrique et la séquence de la sous-unité 1 du gène de la cytochrome c oxydase (gène COI), avec un accent particulier sur les espèces de l'Atlantique Nord. La morphologie de la coquille et son apparence externe ne permettent pas une distinction fiable entre l'espèce bien connue de l'Atlantique nord-est, *A. excavata*, et d'autres espèces ou populations d'*Acesta* de l'Atlantique nord-ouest, à l'exception d'*A. oophaga*. De même, l'analyse de la forme révèle une grande variabilité au sein d'*A. excavata* et un chevauchement morphologique significative avec *A. bullisi* du Golfe du Mexique et *A. rathbuni* du Pacifique sud-ouest et du sud de la Mer de Chine. La forme de la coquille des spécimens de l'Atlantique nord-ouest et nord-central est marginalement similaire à celle d'*A. excavata*. Ces différences sont au moins en partie liées au déplacement antérieur ou postérieur du corps de la coquille et le déplacement opposé de la région dorsale, de la charnière et de la partie supérieure de la lunule. Ces variations morphologiques, ainsi que le ratio de la ligne médiane, expliquent une grande partie de la variabilité extraite par l'analyse en composantes principales. Les résultats de l'approche de code-barres génétique avec l'ADN mitochondrial (COI), cependant, suggèrent que les spécimens de l'Atlantique

nord-ouest appartiennent à une nouvelle espèce pour laquelle nous proposons le nom *Acesta cryptadelphe* **sp. nov.** Les différences dans les tailles de la coquille larvaire entre les spécimens de l'Atlantique nord-est et ceux du nord-ouest supportent ce résultat.

Introduction

Marine hard substrate habitats at bathyal depths in the North Atlantic Ocean are often characterized by the presence of cold-water corals such as *Paragorgia arborea* (Linnaeus), *Primnoa resedaeformis* (Gunnerus) and *Lophelia pertusa* (Linnaeus) (Copley *et al.* 1996; López Correa *et al.* 2005; Sneli *et al.* 2009; Murillo *et al.* 2011). A frequent associate of these deep-water communities is the giant file clam, genus *Acesta* H. Adams & A. Adams, 1858 (Johnson *et al.* 2013; Kenchington *et al.* 2014). In the northeast Atlantic, the European giant file clam, *A. excavata* (J.C. Fabricius, 1779), was the first species of this group to be described (López Correa *et al.* 2005) and, out of *ca.* 30 recent *Acesta* species, it probably has the broadest geographic distribution. Since its original description based on Norwegian specimens (Fabricius 1779), *A. excavata* has been recorded from a wide range of depths (33 to 3200 m) and localities in the northeast Atlantic (Vokes 1963; López Correa *et al.* 2005; Järnegren & Altin 2006), including the North Sea, Iceland and Greenland, the Mediterranean, the continental margin south of Ireland (Johnson *et al.* 2013), the Canary Islands, and along the Mid-Atlantic Ridge, between the Azores and Iceland (Dautzenberg 1927; Copley *et al.* 1996). It also occurs in Pliocene–Pleistocene deposits in the Mediterranean region (López Correa *et al.* 2005).

In the northwest Atlantic, Gagnon & Haedrich (2003) reported the recovery of two *Acesta* specimens from Bay d'Espoir, a deep fjord located along the south coast of Newfoundland (Fig. 1). Based on a general comparison of the shell and soft tissue, they concluded that the Newfoundland specimens were not significantly different from *A. excavata* and probably belong to the same species. The discovery of giant file clams in deep-water canyons along the continental slope off Nova Scotia in 2007 (Fig. 2) (Kenchington *et al.* 2014), and subsequently near Flemish Cap, off the northeast Grand Bank of Newfoundland in 2010, support the suggestion by Gagnon & Haedrich (2003) that the distribution of this group in the northwest Atlantic could be much broader where suitable environments are present. These recent findings, however, prompted the examination of a more extensive sample of North Atlantic material to determine whether the eastern Canadian specimens are part of a much broader distribution of the European giant file clam, *A. excavata*, or whether they constitute a distinct species.

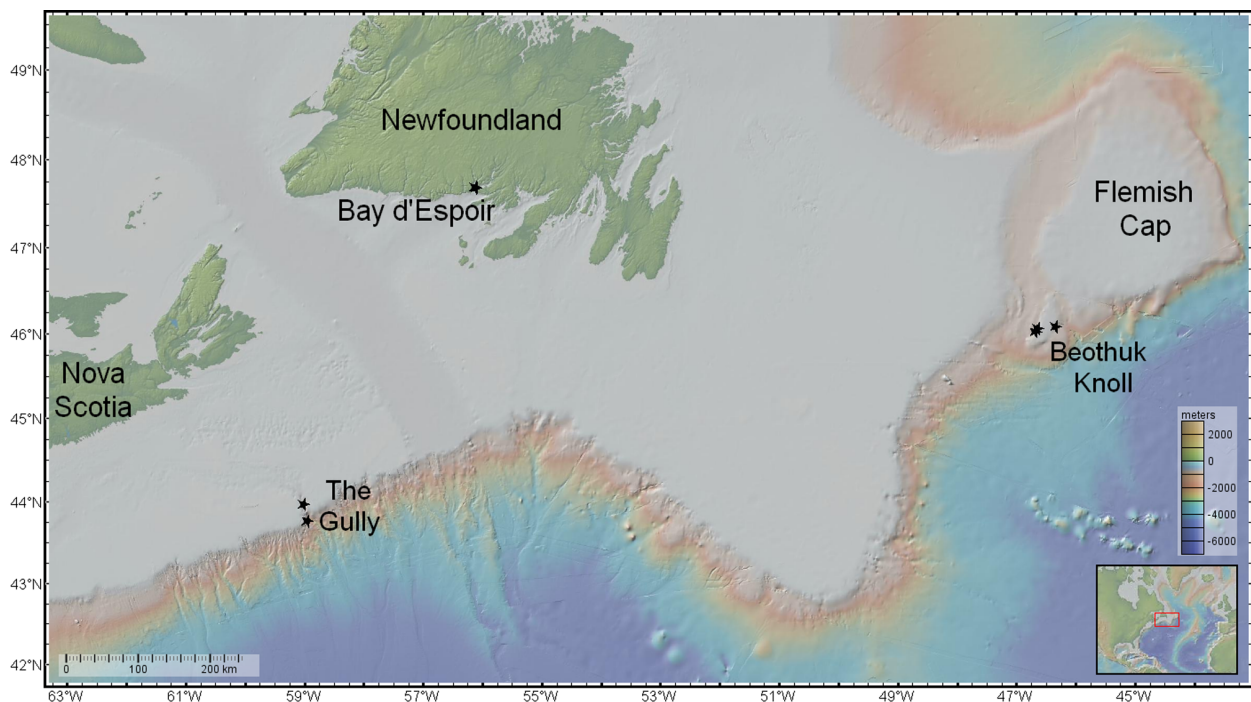


FIGURE 1. Location of the sampling sites where giant file clams (*Acesta*) were collected and observed in the northwest Atlantic. Base map generated with GeoMapApp (<http://www.geomapapp.org>) (Ryan *et al.* 2009).

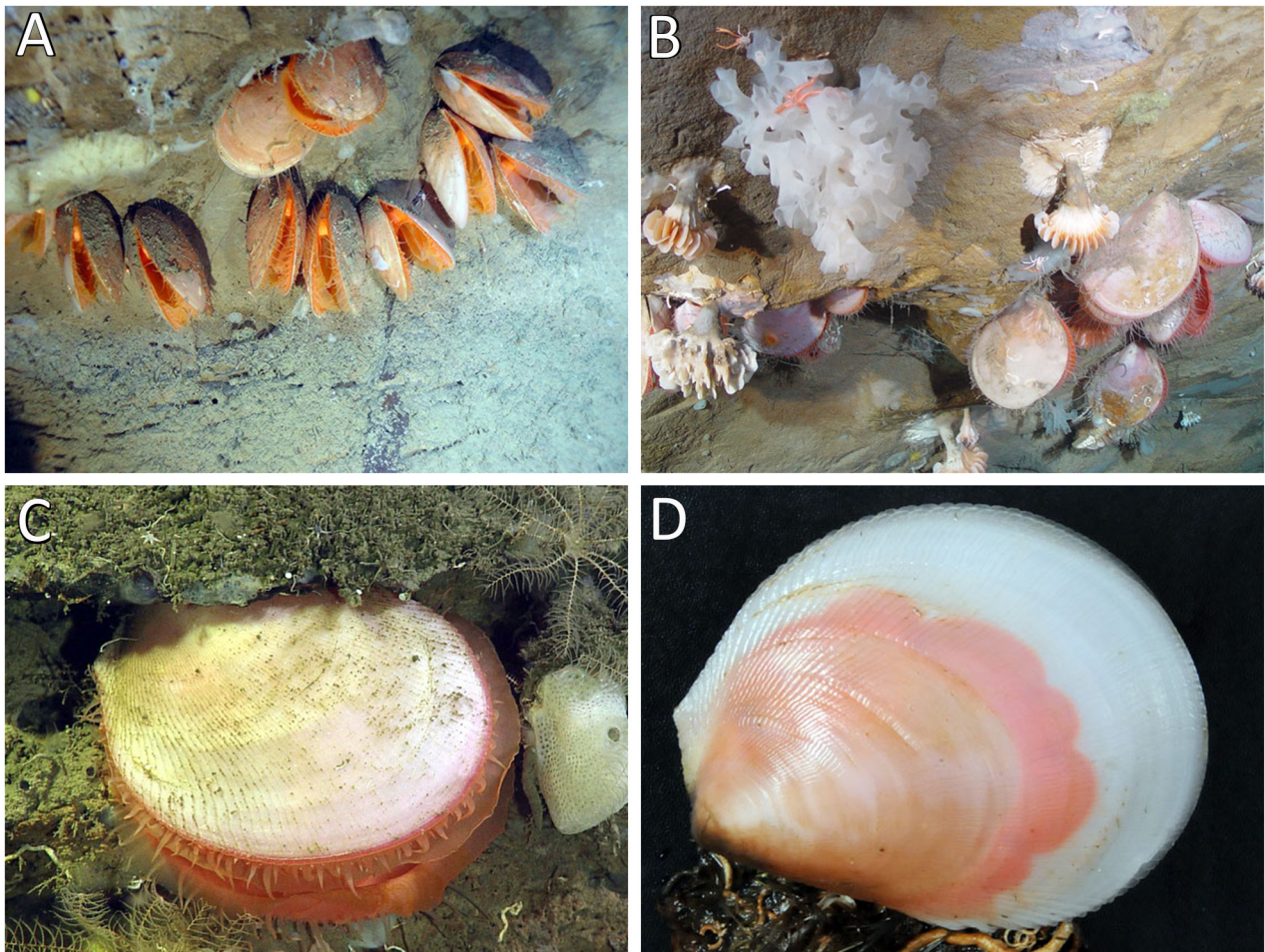


FIGURE 2. (A, B, C) In-situ images of giant file clams, *Acesta* sp., from The Gully, located approximately 200 kilometres off Nova Scotia, to the east of Sable Island, on the edge of the Scotian Shelf. Specimens are assumed to be *A. cryptadelphe* sp. nov. The cup coral and glass sponge in (B) are *Desmophyllum* Ehrenberg and *Asconema* Kent, respectively. The crinoids and glass sponge in (C) are unidentified. (D) Close-up of *A. cryptadelphe* sp. nov. specimen CMNML 097158 freshly collected with the ROPOS ROV.

A cursory examination of a Nova Scotian specimen revealed a shell morphology closer to that of *Acesta bullisi* (Vokes, 1963), one of two species found in the Gulf of Mexico (Järnegren *et al.* 2007), than to that of *A. excavata*. This may have been due to the fact that all of those specimens had a very thin white to semi-translucent shell with a narrower hinge line and smaller v-shaped ligament compared to previously examined *A. excavata*. However, a quantitative comparison with sufficient sample size was necessary in order to draw any firm conclusions. We have obtained thirteen specimens from different localities along the continental slope of eastern Canada, allowing for a better comparison of the shell morphology of the northwestern Atlantic specimens with the European giant file clam and other *Acesta* species such as the two found in the Gulf of Mexico (Järnegren *et al.* 2007).

Very little is known about the soft tissue morphology of *Acesta* species (Gagnon & Haedrich 2003). This leaves us with comparing the shell morphology, particularly in postlarval forms, which is how most shelled mollusc species have typically been distinguished. The challenge, however, is that most *Acesta* shells bear few morphological features that can be used to distinguish species (Figs. 3, 4). Other than the rather unusually shaped *Acesta oophaga* Järnegren, Schander & Young, 2007, the second species from the Gulf of Mexico (Fig. 3F), most species are characterized by the presence or absence of radial ribs (and their prominence when present) on the external side of the valves, the shape and size of the hinge ligament (particularly the oblique v-shaped ligament) and the general shape and profile of the shell. A morphometric comparison of shell shapes has never been performed on this group of bivalves. Kenchington & Full (1994) and Brusoni & Basso (2007) successfully used shell shape analysis to differentiate populations of sea scallops, *Placopecten magellanicus* (Gmelin, 1791) and

subspecies of the astartid *Goodallia triangularis* (Montagu, 1803), respectively. More recently, Leyva-Valencia *et al.* (2012) used the same method to distinguish both species and populations of *Panopea* Ménéard de la Groye, 1897, in the Gulf of California. Here, we hypothesize that *Acesta* specimens found throughout the North Atlantic, including the Gulf of Mexico, show a wide degree of variation in shell shape, resulting in little or no means of easily distinguishing species on a morphometric basis alone (other than *A. oophaga*).

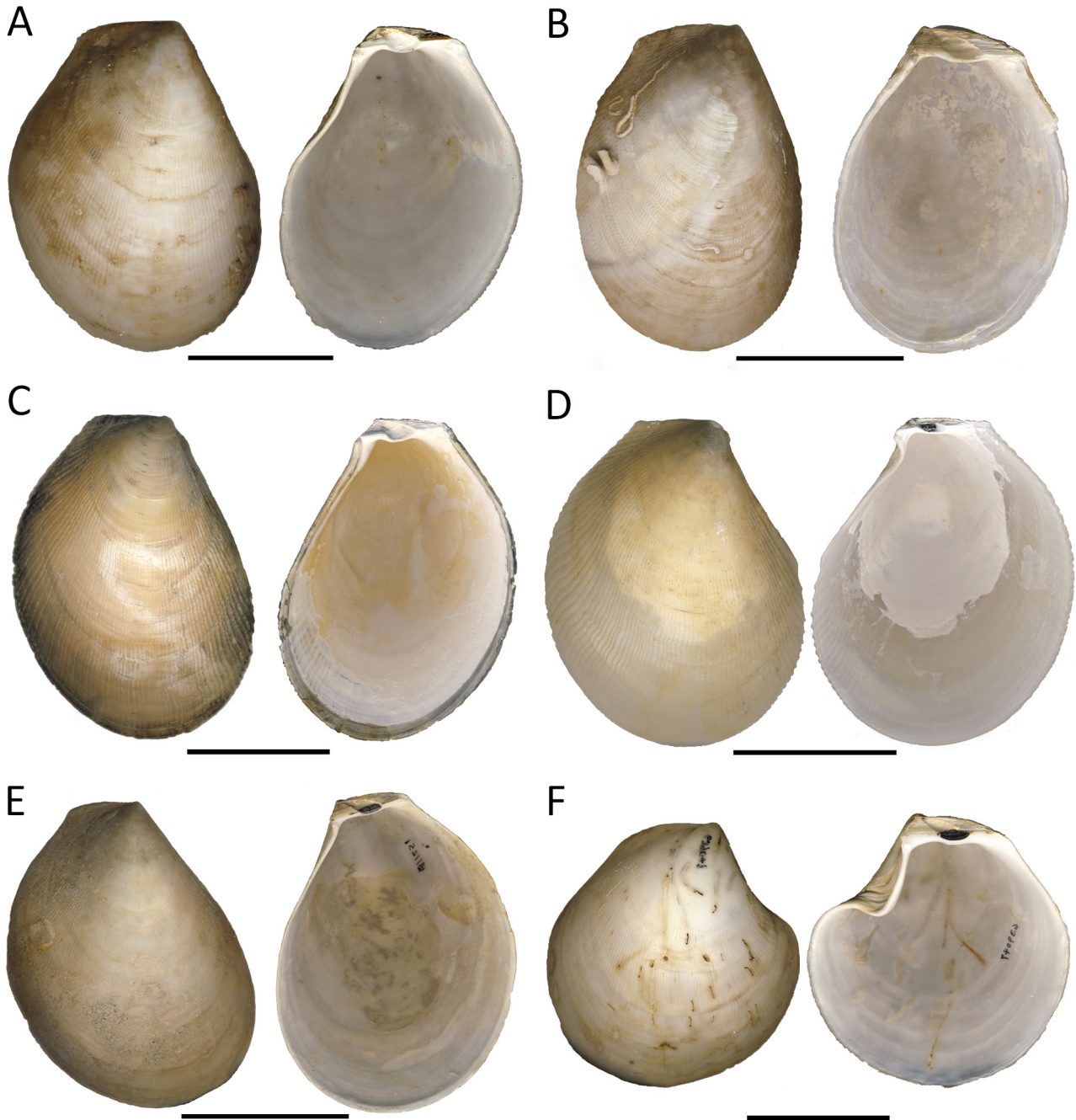


FIGURE 3. External and internal views of the valve of six North Atlantic groups of *Acesta*. (A) *A. excavata*; ZMUC Trondheimsfjord, Norway, 09-1934, right valve. (B) *A. excavata*; The Azores, CMNML 042946, mirror image of left valve. (C) *A. cryptadelphe* **sp. nov.**; Bay d'Espoir, Newfoundland, CMNML 092957, right valve. (D) *A. cryptadelphe* **sp. nov.**; The Gully, northwest Atlantic Ocean, CMNML 097158, right valve. (E) *A. bullisi*; Gulf of Mexico, USNM 811251, mirror image of left valve. (F) *A. oophaga*; Gulf of Mexico, USNM 639047, mirror image of left valve. Scales = 5 cm.

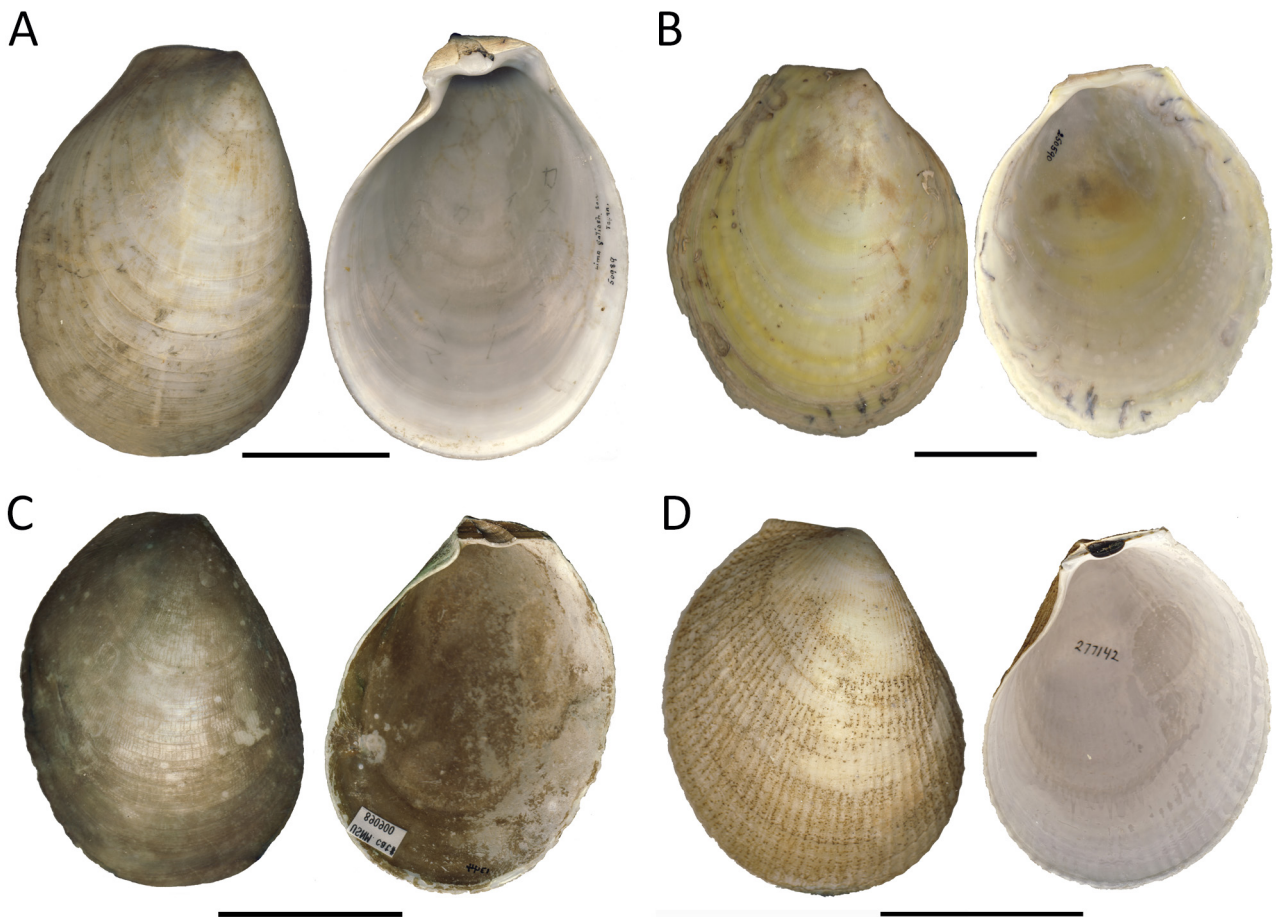


FIGURE 4. External and internal views of the valves of four species of *Acesta* from the South and West Pacific. (A) *A. goliath*; western North Pacific Ocean, AMNH 50989, right valve. (B) *A. rathbuni*; western South Pacific Ocean, AMNH 250590, right valve. (C) *A. saginata*; central South Pacific Ocean, USNM 890900, mirror image of left valve. (D) *A. smithi*; western North Pacific Ocean, AMNH 277142, right valve. Scales = 5 cm.

The morphology and size of the larval shell (prodissoconch) has been used to infer the mode of larval development in marine molluscs (Jablonski & Lutz 1983; Lima & Lutz 1990; Malchus & Sartori 2013) and can sometimes be used to distinguish closely related species (Ockelmann 1965; Redfearn *et al.* 1986). There is little information available, however, on the larval shell morphology or the mode of larval development for the genus *Acesta*. Järnegren *et al.* (2007) reported a larval shell length of 217 μm for one specimen of *A. excavata*. When present, we also examined the general morphology and size of the larval shell of the *Acesta* specimens used in this study.

Increasingly, genetic data is being used for taxonomic hypothesis testing (Hebert *et al.* 2003; Hebert & Gregory 2005) and some authors have even proposed that it takes a central role in framing taxonomic information and defining taxonomic units (Tautz *et al.* 2003). Certainly, genetic data have long been used in integrative taxonomy, along with ecological data, and current practices favour this approach (Goldstein & DeSalle 2011). DNA-based identifications using a portion of the cytochrome oxidase subunit I (COI) mitochondrial protein-coding gene has been employed across broad taxonomic ranges (Hebert *et al.* 2003). This approach has been popularly coined “DNA-barcoding”. Järnegren *et al.* (2007) have recently applied integrative taxonomy to the *Acesta* species in the Gulf of Mexico to identify a new species, *A. oophaga*, distinct from *A. bullisi*. Their analysis includes four mitochondrial genes, 12S, 16S, Cytb, and COI. However, the COI gene is the most suitable for our purposes, showing little or no intraspecific variability and a ten-fold increase in variation among *Acesta* species (Järnegren *et al.* 2007). This is consistent with the expectation that COI gene sequences are also useful for phylogenetic analyses of bivalve molluscs at the species and higher taxonomic levels (Folmer *et al.* 1994). We here apply an integrative taxonomic approach to species circumscription in *Acesta*, using comparative COI gene

sequences in addition to shell morphometrics. We test our hypothesis that sufficient genetic differentiations exist between *Acesta* groups in the northeast and northwest Atlantic and the Gulf of Mexico to warrant the designation of a new species in the northwest Atlantic.

Material and methods

Specimens used for comparative analyses. 152 *Acesta* specimens belonging to seven described species were obtained from seven institutions (Tab. 1). We included species from the western Pacific to provide additional points of comparison in terms of shell morphology. Most of the specimens examined (69%) are *A. excavata* from Norway with a few from Iceland, reflecting the predominance of that species in northeastern American and western European natural history collections. Of the 152 specimens examined, only six still have a measurable larval shell: two *Acesta* specimens from the northwest Atlantic (CMNML 097157.2 and CMNML 097162), and four specimens of *Acesta excavata* from Norway - two from Trondheimsfjord, and two from Hardangerfjord.

Thirteen of the 152 specimens of *Acesta* were collected from the northwest Atlantic (Fig. 1, Tab. 1) from seven locales (Tab. 2). Specifically, four specimens from “The Gully” marine protected area, a deep-water canyon located approximately 200 kilometres off Nova Scotia on the edge of the Scotian Shelf, were collected in 2007 (Fig. 1) and in 2010, using ROPOS, a remotely operated underwater vehicle (ROV) (Kenchington *et al.* 2014) – hereafter referred to as Nova Scotia slope (Tab. 1); two specimens were collected in 1984 and 1985 from Bay d’Espoir, Newfoundland (Gagnon & Haedrich 2003); and seven specimens were collected with a rock dredge in 2010 during the NEREIDA surveys (Durán Muñoz *et al.* 2014) from around Beothuk Knoll, southwest of Flemish Cap and east of Newfoundland – the latter seven specimens hereafter referred to as “Newfoundland slope” (Tab. 1). Five of these samples were appropriately preserved for genetic analyses (Tab. 3). Due to the relative isolation of the mid- and northwest Atlantic specimens from those of the northeast Atlantic, they were not automatically presumed to be *A. excavata* in our study, even though they were identified previously as such for the Azores (see López Correa *et al.* 2005) and for Bay d’Espoir, Newfoundland (Gagnon & Haedrich 2003).

TABLE 1. Geographic and institutional* provenance of the 152 *Acesta* specimens used in this study for the morphometric analyses.

Species	Geographic region	AMNH	UMB	CMN	IRSNB	BIO-DFO	USNM	ZMUC
<i>A. excavata</i>	Norway–Iceland	8	46	1	4		16	30
<i>A. excavata</i>	The Azores			2				
<i>Acesta</i> sp. nov.	Nova Scotia Slope					4		
<i>Acesta</i> sp. nov.	Newfoundland Slope			2		7		
<i>A. bullisi</i>	Gulf of Mexico						3	
<i>A. oophaga</i>	Gulf of Mexico						5	
<i>A. goliath</i>	Japan	1						
<i>A. rathbuni</i>	South Pacific, South China Sea, Philippines	3					17	
<i>A. saginata</i>	South Pacific						2	
<i>A. smithi</i>	Japan	1						

* AMNH: American Museum of Natural History; UMB: Natural History Collections–Norwegian University of Life-sciences; CMN: Canadian Museum of Nature; IRSNB: Royal Belgian Institute of Natural Sciences; BIO-DFO: Bedford Institute of Oceanography—Department of Fisheries and Oceans Canada; USNM: National Museum of Natural History—Smithsonian Institution; ZMUC: Zoologisk Museum—University of Copenhagen.

Shell imaging. There are few structures in adult shells for between-species comparisons other than the dorsal hinge with its oblique v-shaped ligament pit and the inner margin of the hinge plate (Fig. 5). External radial ribs, particularly visible in the anterior and posterior regions of *A. excavata*’s valves, represent at best a qualitative character not shared by many species (Figs. 3, 4). In this study, all shells were examined qualitatively to assess the degree of variation in form and arrangement of radial ribs on their external surface.

TABLE 2. Collection details of *Acesta* sample sets from the northwest Atlantic.

Set	Cruise	Sampler	Sample/ Dive #	Sampling date
1	DAWSON 84-050	van Veen Grab	BdE 14.1	10-Dec-1984
2	PANDORA II	PISCES IV Sub	1629	26-Jun-1985
3	HUDSON 2007-025	ROPOS ROV	1057	10-Jul-2007
4	NEREIDA 0610	Rock dredge	DR68-01	24-Jun-2010
5	NEREIDA 0610	Rock dredge	DR71-47	27-Jun-2010
6	NEREIDA 0610	Rock dredge	DR72-02	28-Jun-2010
7	HUDSON 2010-029	ROPOS ROV	1334-4	9-Jul-2010

continued.

Set	Collector	Location	Latitude / Longitude	Water depth (m)
1	J.-M. Gagnon	Bay d'Espoir	47°40'48"N, 56°06'30"W	600–700
2	J.-M. Gagnon	Bay d'Espoir	47°41'12"N, 56°07'36"W	750
3	E. Kenchington	The Gully	43°46'01.1"N, 59°57'18.8"W	1241
4	F.J. Murillo	Beothuk Knoll	46°03'42.8"N, 46°38'29"W	745
5	F.J. Murillo	Beothuk Knoll	46°04'47.9"N, 46°20'31.4"W	888
6	F.J. Murillo	Beothuk Knoll	46°01'26.2"N, 46°41'11.2"W	710
7	E. Kenchington	The Gully	43°58'06"N, 59°01'03"W	680

With this constraint in mind, while qualitatively comparing the external shell features for all specimens, this study concentrates on the adult shell shape. The latter is defined by the outline represented by the linear configuration of the internal edge of the hinge and the external margin of the anterior, ventral and posterior regions of the valve (Fig. 5). In order to obtain consistent images of this “outline” suitable for subsequent digital processing, the internal surface of the right valve of each specimen was scanned in TIFF using a high resolution (1200 x 1200 dpi) flatbed scanner (Canon CanoScan 4400F). Where the right valve was unavailable, the mirror image of the left valve was used instead because the two valves are virtually identical. Two rulers were placed horizontally and vertically alongside each shell to provide a scale (in mm). This also allowed confirmation that the shell image was not distorted by the scanning process. The single valve inflation was measured directly with a calliper. The external side of each valve was also scanned to observe external features; these images cannot be used quantitatively because of significant distortion as most of the shell's outer surface is not in contact with the flat surface of the scanner.

The larval shell (prodissoconch) on the two specimens from the northwest Atlantic was photographed and measured under an Olympus SZX12 stereomicroscope, at 108x magnification (i.e., 90x and 1.2x objective). Four specimens of *Acesta excavata* from Norway (two from UMB, two from ZMUC) still had a visible larval shell, and images of the larval shells, with scales, were provided by the corresponding institutions.

Landmark and semilandmark definitions. The internal image of each valve was used to obtain landmarks from the 2-D outline for geometric morphometrics analysis. As indicated above, the positioning of landmarks on the outline of *Acesta* shells is greatly limited by the lack of distinctive structures, with the exception of the shell hinge. By definition, landmarks must be homologous between specimens (Zelditch *et al.* 2012). Landmarks 1 to 5 (LM-1, etc.) are positioned along the inner margin of the hinge plate of each shell, hereafter referred to as the hinge line (Fig. 5): LM-1 is located at the most anterior point of the hinge line; LM-2 is the point of contact between the inner edge of the anterior hinge line and the anterior margin of the central v-shaped ligament pit; LM-4 is the point of contact between the inner edge of the posterior hinge line and the posterior margin of the v-shaped ligament pit; LM-5 is located at the most posterior point of the posterior hinge line; and LM-3 is defined as the midpoint between LM-2 and LM-4. These five landmarks define the inner edge of the hinge line. The accurate positioning of this line is critical for the subsequent positioning of semilandmarks along the shell margin. The dorsal portion of the shell situated above the hinge line (Fig. 5) was not considered in this study; in addition to being in the third dimension, it typically reflects increasing thickness of the shell in older specimens (López Correa *et al.* 2005).

TABLE 3. Details of *Acesta cryptadelphe* sp. nov. type series from the northwest Atlantic, with shell measurements and the GenBank accession numbers.

Catalogue number*	Type	NCBI GenBank accession #	Sample set**	Shell length (cm)	Shell width (cm)	Hinge length (cm)	Shell half inflation (cm)	Midline width ratio	Preservation note
CMNML 097156	Holotype	KR706466	3	9.1	6.8	2.9	1.95	0.554	tissue and right valve preserved in 70% ethanol, left valve dry
CMNML 097157.1	Paratype 1	-	3	10.1	8.1	2.5	2.0	0.661	tissue preserved in 70% ethanol, valves dry
CMNML 097157.2	Paratype 2	-	3	9.9	7.4	2.7	2.0	0.545	tissue preserved in 70% ethanol, valves dry
CMNML 097158	Paratype	KR706467	7	10.0	8.1	2.9	1.9	0.576	tissue and left valve preserved in 70% ethanol, right valve dry
CMNML 097159.1	Paratype 1	-	4	10.7	8.8	2.8	2.15	0.588	left valve dry
CMNML 097159.2	Paratype 2	-	4	11.4	8.7	2.9	2.45	0.628	right valve and part of left valve dry
CMNML 097159.3	Paratype	KR706464	4	-	-	-	-	-	Tissue preserved in 90% ethanol, separated from valves
CMNML 097159.4	Paratype	KR706468	4	-	-	-	-	-	Tissue preserved in 90% ethanol, separated from valves
CMNML 097160.1	Paratype 1	KR706465	6	12.7	9.6	3.4	2.5	0.614	left valve dry
CMNML 097160.2	Paratype 2	-	6	10.7	8.1	2.9	2.1	0.458	tissue in 70% ethanol, left valve dry
CMNML 097161.1	Paratype 1	-	6	13.0	10.2	3.1	3.0	0.732	left valve dry
CMNML 097161.2	Paratype 2	-	6	12.7	10.3	3.2	3.2	0.656	left valve dry
CMNML 097162	Paratype	-	5	1.4	1.1	0.4	0.2	0.716	left valve dry
CMNML 092957	Paratype	-	1	11.2	8.3	3.0	2.4	0.729	right valve dry
CMNML 092958	Paratype	-	2	11.1	9.3	3.4	2.55	0.584	tissue and right valve preserved in 70% ethanol, left valve dry

* Deposited at the Canadian Museum of Nature, Mollusc Collection.

** See Table 1 for the Sample Set descriptions.

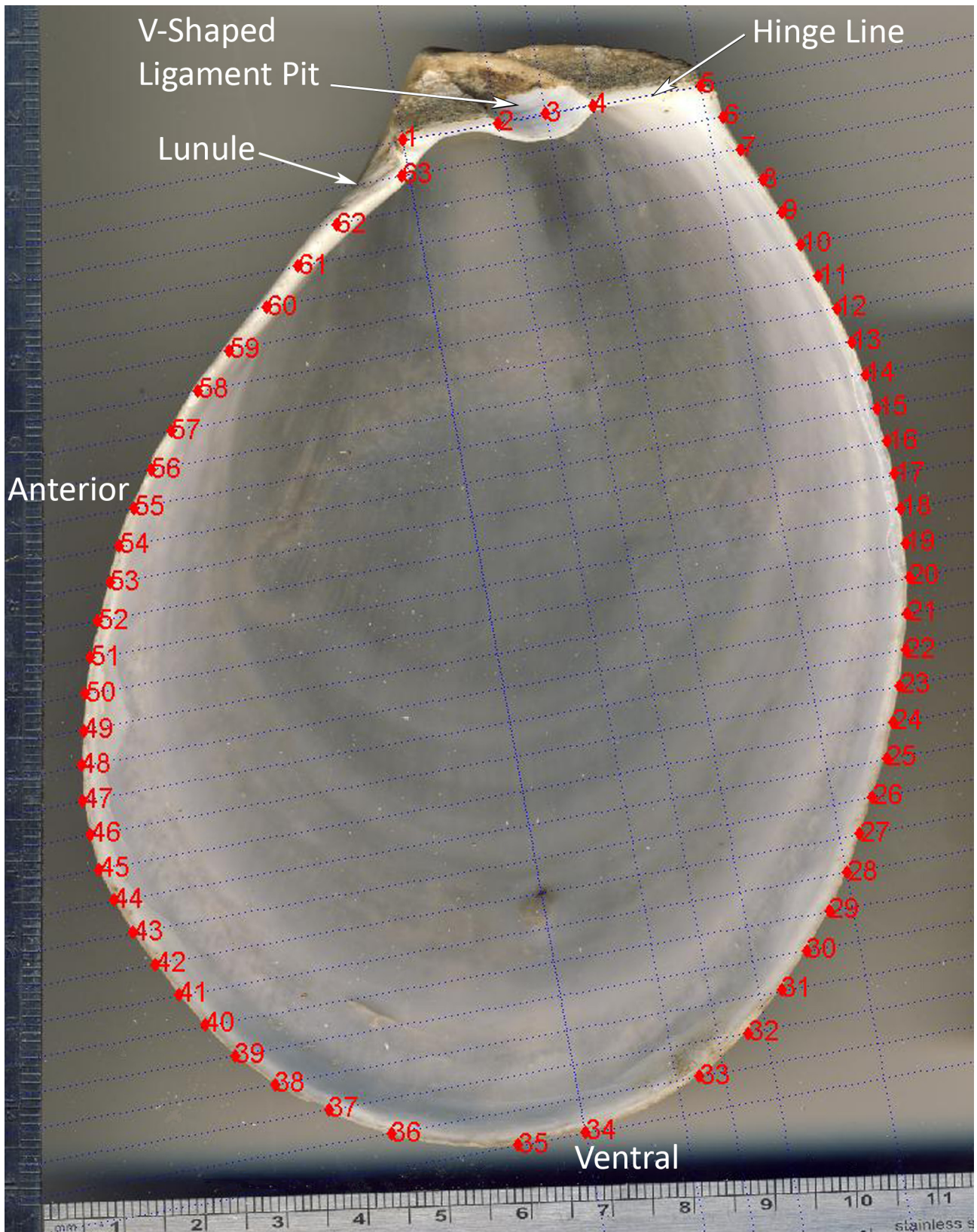


FIGURE 5. Inside view of a right valve of *Acesta excavata*, showing morphological features, landmarks 1 to 5 and 58 semilandmarks (6 to 63) positioned where the lines from the superimposed comb intersect the shell margin.

Semilandmarks are points that are intended to capture complex curving morphologies, particularly when landmarks are sparse (Bookstein 1997). The number of semilandmark points is arbitrary but it is understood that the greater the number, the more accurate is the curve summary (Webster & Sheets 2010). In order to position the

semilandmarks, a perpendicular line to the hinge line was drawn from LM-1 (Fig. 5) using the program MakeFan7 (Sheets 2004). From LM-1 to the intersect point between the perpendicular line and the ventral edge of the shell, a comb was drawn with a total of 30 lines, also using MakeFan7. This resulted in 58 distinct and reasonably spaced semilandmarks where each line intersected the shell margin. This approach seemed to provide a more uniform coverage of the shell outline than most fan configurations. MakeFan7 was used to digitize the landmarks and semilandmarks and produce data files used for subsequent analyses.

Size measurements and ratios. We extracted the lunule length, hinge length and shell length (Fig. 5), based on the landmarks and semilandmarks obtained from the images for each *Acesta* specimen (with the incorporated scales). Valve inflation was measured directly. The shell width was measured along the midline between semilandmarks (SML) 20 and 49. The distances between each of these two semilandmarks and the intersect point to the perpendicular line drawn from LM-1 are also calculated. A number of ratios are derived from these measurements: lunule length/hinge length, lunule length/shell length, hinge length/shell length, shell width/shell length, and distance from SML-49 to midline intersect/distance from SLM-20 to midline intersect. This last ratio is here called the midline-width-ratio which represents the anteroposterior proportion of the shell along the midline. The statistical package PAST (Hammer 2014) was used to test differences in slopes (analysis of covariance, ANCOVA) and in distribution along the midline-width-ratio between taxa (Mann-Whitney U test).

Shell shape analyses. Each shell dataset is made up of XY coordinates for the 5 landmarks and 58 semilandmarks. The location, scale (size) and rotation of each set of landmarks and semilandmarks were first adjusted to allow size-independent comparison of all shell shapes (Kendall 1984) by removing allometric effects (Parr *et al.* 2011). A number of superimposition techniques are available in geometric morphometrics to do this; we used Partial Procrustes Superimposition (Rohlf 1999). In Partial Procrustes Superimposition, all points are treated equally, whereby the reference form is rescaled to have a set centroid size and a position of zero (Webster & Sheets 2010). This provides a mean form that is repeatedly rotated and realigned until the mean shape does not significantly change (Rohlf 1999). The program CoordGen7 (Sheets 2003) was used for this process.

The program SemiLand6 (Sheets 2002) was used to reduce the bending energy by sliding the semilandmarks along the curve until optimally spaced (Bookstein 1997; Webster & Sheets 2010). The resulting landmark and corrected semilandmark data were then analyzed with PCAGen7 (Sheets 2001) to examine the variance in shell shapes by performing principal component analysis (PCA). It is also a means to identify potential outliers and groupings in the data (Webster & Sheets 2010). With the majority of the specimens in this study being *Acesta excavata* (N = 105), a separate PCA was also performed to examine its within-species variance in shape. Thin-plate spline deformation grids are used to depict changes in shape along the principal components (Perez *et al.* 2006).

The program CVAGen6 was used to perform Canonical Variates Analysis (CVA) based on partial warp scores (Sheets 2006). CVA determines a set of axes that best discriminate between two or more groups/species in the data (Sheets *et al.* 2006). CVAGen computes the canonical variates scores of all the specimens and uses Mahalanobis distances to assign them to groups (Sheets 2006). For this reason, all species groups with less than 3 specimens have to be removed: *Acesta excavata* from the Azores, *A. smithi* (G.B. Sowerby III, 1888), *A. goliath* (G.B. Sowerby III, 1883) and *A. saginata* Marshall, 2001. By doing so, assignment and jackknife tests can be performed within the CVAGen program to determine the effectiveness of group assignment. The procedure used takes 10% of the specimens and assigns them as unknowns over 1000 trials to identify whether they are correctly placed within groupings and whether these assignments are significant. However, with a dataset of a relatively low sample number (146 specimens) in relation to 126 XY values (descriptors) for the Procrustes coordinates, the number of descriptors was deemed too high to properly extract canonical multivariate trends (H.D. Sheets, pers. comm.). To address this issue, the CVA was performed on fewer multivariate axes by using the PCA reduction option in CVAGen; i.e., the first 10 PCA components were used to represent the main gradients/trends in the dataset instead of the 126 XY values. The resulting CVA scores were plotted for the first three axes. As with the PCA, the CVA-derived deformation grids (in Procrustes Superposition) were produced for the extremities of each CVA axis. The above approach was repeated but with the Newfoundland and Nova Scotia specimens included as unknowns in the CVAGen program to determine their assignment by the CVA relative to the other *Acesta* groups.

Genetic analyses. Genomic DNA was extracted from mantle tissue of five *Acesta* specimens from the northwest Atlantic (Tab. 3) using a Qiagen DNeasy isolation kit. A portion of the COI gene of approximately 710 bp was amplified using universal primers LCO1490 (5'-GGTCAACAAATCATAAAGATATTGG-3') and HCO2198 (5'-TAAACTTCAGGGTGACCAAAAAATCA-3') (Folmer *et al.* 1994) or dgLCO-1490 (5'-GGTCAACAAATCATAAAGAYATYGG-3') and dgHCO-2198 (5'-TAAACTTCAGGGTGACCAARAAYCA-

3') (Meyer 2003). The PCR volume was 25 µl consisting of 10X ThermoPol Reaction Buffer, 200 µM each dNTP, 0.5 µM of each primers, 2.5 mM MgCl₂, 0.5 units of Taq DNA polymerase (NEB), 4 µl of DNA template and Milli-Q water for the remainder. The PCR thermal protocol was a single cycle of 94°C/2 min, followed by 5 cycles of 94°C/1 min, 45°C/90 s, 72°C/90 s. This was followed by 35 cycles of 94°C/1 min, 50°C/90 s, 72°C/1 min and a final elongation step of 72°C/5 min. The PCR product was visualized on a 1% agarose gel stained with SYBR Safe DNA Gel stain (Life Technologies). The product was cleaned using the Shrimp Alkaline Phosphatase (SAP) protocol to remove excess primer and dNTPs, and sequenced in both forward and reverse directions with complete overlap by Genewiz Inc. (South Plainfield, NJ).

Fifty-nine partial COI gene sequences from five species of *Acesta* and three other genera of Limidae were retrieved from the GenBank Nucleotide database of NCBI (www.ncbi.nlm.nih.gov) (Tab. 4). This data set includes all available sequences of this gene for *Acesta* spp. to date, with the exception of four sequences of *A. sphoni* (Hertlein 1963) which were excluded as they are only 375 bp in length. The *Acesta* sequences, including the five new sequences generated by this study (Tab. 3) were trimmed at the 5' and 3' ends to equal length (586 bp). This data set has no insertions/deletions. All sequences were then aligned using the Clustal Omega multiple sequences algorithm at EMBL (<http://www.ebi.ac.uk/Tools/msa/clustalo/>) (McWilliam *et al.* 2013) to incorporate the *Lima* Bruguière, 1797 and *Limaria* Link, 1807 taxa that were used as an out-group for the analyses. This second alignment was used to trim the *Lima* and *Limaria* sequences. A final alignment was produced using all sequences, allowing for gaps to be introduced.

TABLE 4. Taxa from other studies used in phylogenetic analyses, with NCBI GenBank accession numbers.

Species	N	Accession numbers
<i>Acesta bullisi</i> (Vokes, 1963)	3	AM494905.1, AM494906.1, AM494907.1
<i>Acesta excavata</i> (J.C. Fabricius, 1779)	4	AM494908.1, AM494909.1, AM494910.1, AM494911.1
<i>Acesta oophaga</i> Järnegren, Schander & Young, 2007	5	AM494900.1, AM494901.1, AM494902.1, AM494903.1, AM494904.1
<i>Acesta sphoni</i> (Hertlein, 1963)	4	EF460405.2, EF460406.2, EF460407.2, EF460408.2
<i>Acesta mori</i> (Hertlein, 1952)	40	EF460461.2, EF460459.2, EF460457.2, EF460456.2, EF460454.2, EF460453.2, EF460451.2, EF460450.2, EF460449.2, EF460448.2, EF460447.2, EF460446.2, EF460444.2, EF460443.2, EF460439.2, EF460438.2, EF460432.2, EF460431.2, EF460428.2, EF460427.2, EF460426.2, EF460420.2, EF460416.2, EF460415.2, EF460413.2, EF460412.2, EF460442.1, EF460436.1, EF460435.1, EF460434.1, EF460429.1, EF460425.1, EF460424.1, EF460423.1, EF460421.1, EF460418.1, EF460417.1 [PopSet 291165259]; KJ147472.1, KJ147473.1, KJ147474.1 [PopSet: 602219171 partial]
<i>Limaria loscombi</i> (G.B. Sowerby I, 1823)[syn. <i>Lima loscombi</i> G.B. Sowerby I, 1823; <i>Limea loscombii</i> (G.B. Sowerby I, 1823)]	1	AM494912.1
<i>Lima lima</i> (Linnaeus, 1758)	1	AF120649.1
<i>Limaria hians</i> (Gmelin, 1791)	1	AF120650.1

The partial COI gene sequences were used to position the unknown specimens of *Acesta* collected from the northwest Atlantic (Tab. 3) relative to known species of *Acesta*, *Lima* and *Limaria* (Tab. 4). Their evolutionary history was inferred by using the Maximum Likelihood (ML) method (Tamura *et al.* 2004) based on the Tamura–Nei model (Tamura & Nei 1993). Initial tree(s) for the heuristic search were obtained automatically by applying Neighbor–Join and BioNJ algorithms to a matrix of pairwise distances estimated using the Maximum Composite Likelihood (MCL) approach, and then selecting the topology with superior log likelihood value. A comparative evolutionary history was inferred using the Maximum Parsimony (MP) method. The MP tree was obtained using the Subtree-Pruning-Regrafting (SPR) algorithm (Nei & Kumar 2000) with search level 0 in which the initial trees were obtained by the random addition of sequences (100 replicates). Evolutionary analyses were conducted in

MEGA6 (Tamura *et al.* 2013). In both analyses codon positions included were 1st+2nd+3rd+Noncoding, and all positions containing gaps were eliminated. There were a total of 586 positions in the final dataset.

Results

Adult shell sculptures. The vast majority of the 105 *Acesta excavata* specimens display weak radial ribs in the anterior and posterior regions of the shell, and smoothing of those in the medial region (Fig. 3A–B). There is, however, a fair degree of variability, with some shells having more or less accentuated radial ribs than others. Few specimens appear to have narrower, more numerous radials in the medial region. As observed by López Correa *et al.* (2005), the lunular field is excavated and sometimes slightly gaping to form the byssal notch. There is also much variability in this character, with the lunule being greatly reduced in some cases.

The thirteen Newfoundland and Nova Scotia specimens, as well as the two Azorean specimens, display similar radial rib and lunule patterns and variation to those of *Acesta excavata* (Fig. 3B–D). *Acesta bullisi* also shows similar radial rib patterns but our small sample size ($N = 3$) does not permit generalization. The other Gulf of Mexico resident, *A. oophaga*, has distinctively more uniform (in width and elevation) and broader radials throughout the shell surface (Fig. 3F).

The specimens of the western Pacific species *Acesta rathbuni* (Bartsch, 1913) have a smooth, yellowish shell without radials (Fig. 4B) while *A. goliath* has only a few anterior radial ribs and no distinguishable radials along the medial region (Fig. 4A). *Acesta smithi* displays the most prominent radials, which are fairly uniform in size across the entire shell and even visible internally (Fig. 4D). The two specimens of *A. saginata* (USNM 890900) examined in this study are from the Eltanin Fracture Zone, South Pacific; their rib pattern is indistinguishable from that of *A. excavata* (Fig. 4C).

Larval shell. The prodissoconch (Fig. 6) is dome-shaped, subcircular, and has a uniform glossy surface. Under the light microscope, the shells seem to lack a prodissoconch 2 stage, so this is apparently a shell type 2D following the framework for early ontogenetic shell typology proposed by Malchus & Sartori (2013). However, Figure 6B shows an inner “dirt line” which could represent a P1/P2 boundary. If this were the case, the larval shell should be typified as ST-2C. In any case, the overall larval shell length varies between 241 and 261 μm for the northwest Atlantic specimens and between 203 and 212 μm for the Norwegian specimens (Tab. 5).

TABLE 5. Comparisons of larval shell sizes for six *Acesta* specimens from Norway fjords and the northwest Atlantic.

Species	Catalogue number	Geographic location	Water depth (m)	Whole shell length (cm)	Valve	Larval shell length (μm)
<i>Acesta excavata</i> (Norway)	UMB 4979	Tysnes, Hardangerfjord	300–600	1.3	right	209–212
	UMB 67637	Utne, Hardangerfjord	?	3.0	right	212
	ZMUC BIV-218	Trondheimsfjord	?	4.0	left	203–205
	ZMUC BIV-219	Trondheimsfjord	?	5.5	left	206
<i>Acesta</i> sp. nov. (northwest Atlantic)	CMNML 097157.2	The Gully	1241	9.9	left	256–258
					right	241–261
	CMNML 097162	Beothuk Knoll	888	1.1	left	247–248

Adult shell size measurements and ratios. Shell width vs. shell length (Fig. 7A) shows the strongest linear relationship with no significant difference in slopes between species, except for *Acesta oophaga* (ANCOVA: $df = 108$, $F = 7.8$, $p = 0.006$), which is typically shorter-wider in proportion than *A. excavata*. The hinge length vs. shell length relationship (Fig. 7B) shows the second strongest linear trend, but with species slopes not significantly different from one another. The lunule length vs. shell length (Fig. 7C) shows a linear relationship for most species, but with increasing variation with size and no significant difference in slopes between species, even for *A. rathbuni* which appear to have a proportionally shorter lunule than the other species. A very similar relationship is found for

all species when comparing the lunule length to the hinge length (Fig. 7D), but with *A. excavata* and *A. rathbuni* showing a significant difference in slopes (ANCOVA: df = 123, F = 3.97, p = 0.049).

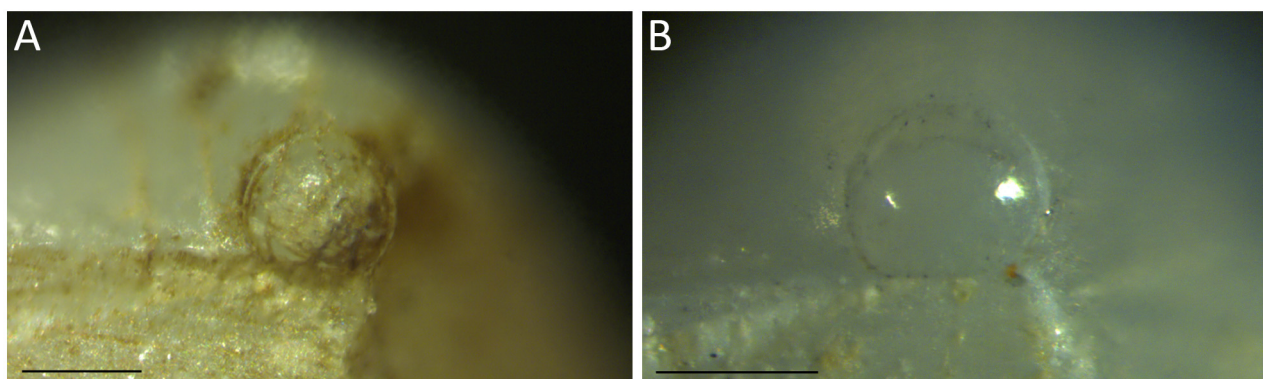


FIGURE 6. Larval shells of *Acesta cryptadelphe* sp. nov. from the northwest Atlantic, viewed under high-magnification stereomicroscope. (A) The Gully, CMNML 097157.2, left valve (same as Fig. 16A). (B) Beothuk Knoll, CMNML 097162, left valve (same as Fig. 15B). Scales = 200 μ m.

The valve inflation against shell length (Fig. 7E) shows a linear relationship except for *Acesta oophaga*, which has a higher and increasing inflation ratio with size than *A. excavata* (ANCOVA: df = 108, F = 11.26, p = 0.001) and the Newfoundland and Nova Scotia specimens (ANCOVA: df = 16, F = 10.36, p < 0.006). Non linearity of this ratio in *A. oophaga* is possibly based on a small sample size (N = 5). *Acesta rathbuni* shows a significant difference in slopes when compared to *A. excavata* (ANCOVA: df = 123, F = 11.3, p = 0.001) and to the Newfoundland and Nova Scotia specimens (ANCOVA: df = 31, F = 10.36, p = 0.006).

The midline-width-ratio does not show a linear relationship with shell length. However, when considering this ratio alone (Fig. 7F, Y-axis), Newfoundland and Nova Scotia specimens as well as those of *Acesta oophaga*, the large *A. rathbuni*, and those from the Azores tend to separate from the bulk of *A. excavata* specimens (lower portion of Fig. 7F). This suggests that the shell of *A. excavata*, along with that of *A. bullisi*, tend to be proportionally more anteriorly elongated. Table 6 summarizes shell morphological ratios for all species and groups of *Acesta* examined in this study.

TABLE 6. Mean \pm standard deviation of shell morphological ratios for all species and groups of *Acesta* examined in this study.

	N	Shell Width / Shell Length	Lunule Length / Shell Length	Hinge Length / Shell Length	Lunule Length / Hinge Length	Half Inflation / Shell Length	Width Ratio
<i>A. excavata</i>	105	0.828 \pm 0.038	0.364 \pm 0.096	0.289 \pm 0.035	1.270 \pm 0.358	0.226 \pm 0.024	0.842 \pm 0.113
Azores	2	0.791 \pm 0.003	0.428 \pm 0.081	0.318 \pm 0.035	1.368 \pm 0.405	0.230 \pm 0.017	0.501 \pm 0.029
Nova Scotia	4	0.845 \pm 0.099	0.486 \pm 0.054	0.294 \pm 0.046	1.675 \pm 0.248	0.221 \pm 0.016	0.584 \pm 0.053
Newfoundland	9	0.838 \pm 0.046	0.407 \pm 0.122	0.274 \pm 0.023	1.503 \pm 0.487	0.222 \pm 0.035	0.634 \pm 0.088
NF+NS*	13	0.840 \pm 0.062	0.432 \pm 0.110	0.280 \pm 0.031	1.556 \pm 0.425	0.219 \pm 0.030	0.619 \pm 0.080
<i>A. bullisi</i>	3	0.832 \pm 0.023	0.342 \pm 0.112	0.267 \pm 0.036	1.325 \pm 0.532	0.216 \pm 0.030	0.825 \pm 0.114
<i>A. oophaga</i>	5	0.972 \pm 0.064	0.379 \pm 0.077	0.319 \pm 0.049	1.232 \pm 0.380	0.239 \pm 0.061	0.613 \pm 0.042
<i>A. rathbuni</i>	20	0.825 \pm 0.035	0.231 \pm 0.067	0.283 \pm 0.038	0.832 \pm 0.280	0.175 \pm 0.013	0.731 \pm 0.105
<i>A. goliath</i>	1	0.801 \pm 0.0	0.243 \pm 0.0	0.277 \pm 0.0	0.875 \pm 0.0	0.194 \pm 0.0	0.989 \pm 0.0
<i>A. saginata</i>	2	0.844 \pm 0.71	0.299 \pm 0.071	0.270 \pm 0.031	1.099 \pm 0.137	0.233 \pm 0.002	0.792 \pm 0.122
<i>A. smithi</i>	1	0.904 \pm 0.0	0.201 \pm 0.0	0.325 \pm 0.0	0.617 \pm 0.0	0.254 \pm 0.0	0.855 \pm 0.0

* *Acesta* specimens from Newfoundland & Nova Scotia, NW Atlantic (*A. cryptadelphe* sp. nov.).

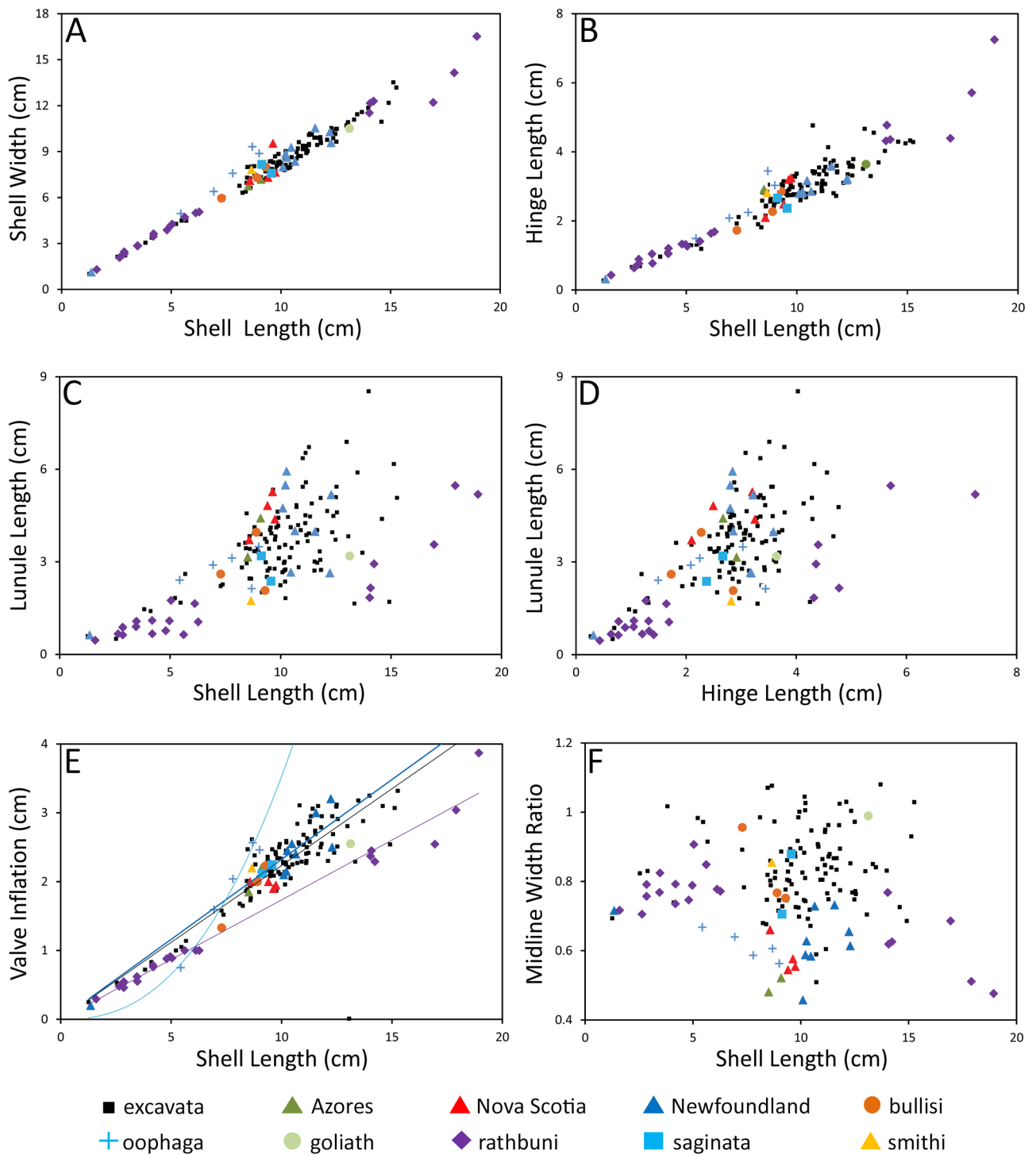


FIGURE 7. Scatter plots comparing various shell measurements and ratio for the ten different groups of *Acesta* examined in this study. Regression lines in (E) are shown for *A. excavata* (black line), the Newfoundland group (blue line), *A. rathbuni* (purple line) and *A. oophaga* (light blue power-function curve); intersect is set at 0 for all regressions.

The non-parametric Mann-Whitney U tests support significant differences in midline-width-ratio between *Acesta excavata* (N = 105) and Newfoundland specimens (U = 101, N = 9, $p < 0.0001$), Nova Scotia specimens (U = 8, N = 4, $p < 0.001$), the Azores specimens (U = 2, N = 2, $p < 0.023$), *A. oophaga* (U = 16, N = 5, $p < 0.0004$) and *A. rathbuni* (U = 520, N = 20, $p < 0.0003$). However, the sequential Bonferroni corrected significance (applied when performing repeated tests) only supports significant differences between *A. excavata* and the Newfoundland specimens ($p < 0.0006$), *A. oophaga* ($p < 0.015$), *A. rathbuni* ($p < 0.011$) and Nova Scotia specimens ($p < 0.047$).

Landmarks and semilandmarks. Figure 8A shows a plot of the Procrustes coordinates for the 5 landmarks (black) and 58 corrected semilandmarks (blue), for all 152 specimens. A fair amount of variability is observed over all landmarks and semilandmarks but particularly around the lunule (upper left area of the shell outline of Fig. 8A). Some of the most variable points in that region reflect the particular shape of *Acesta oophaga*, with its deeply concave lunule (Fig. 3F). Figure 8B shows the landmarks and corrected semilandmarks for *A. excavata* alone. While the scatter of points around each landmark and semilandmark is more compact, particularly with the absence of *A. oophaga* points, it shows a fair amount of shape variation within this species.

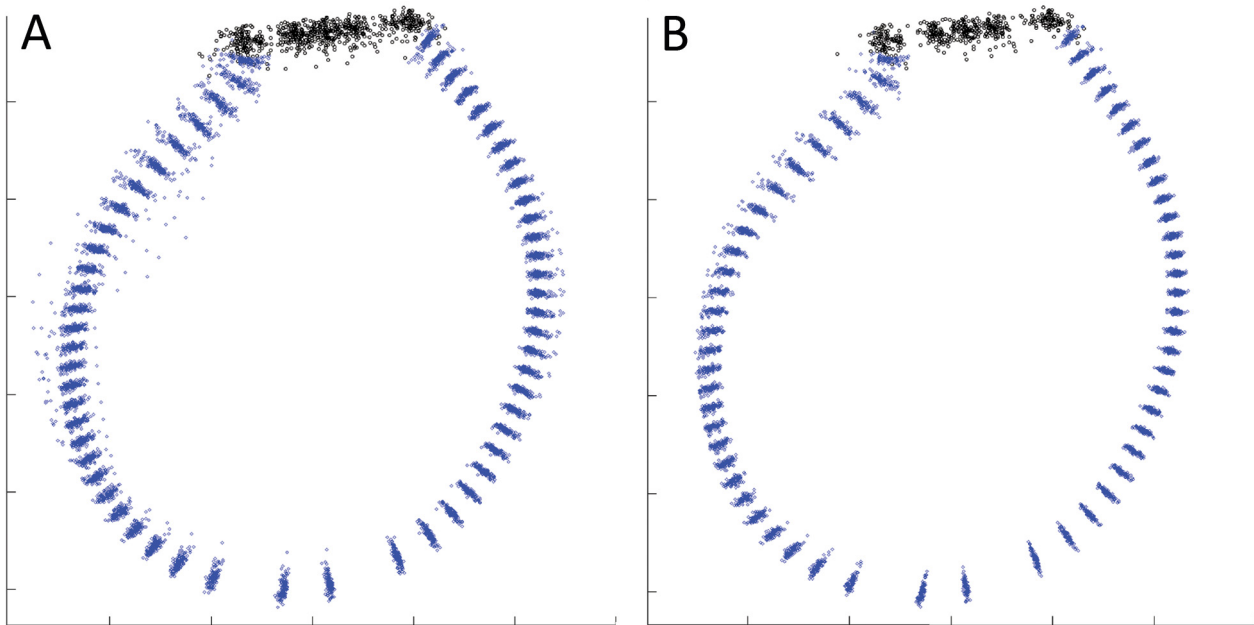


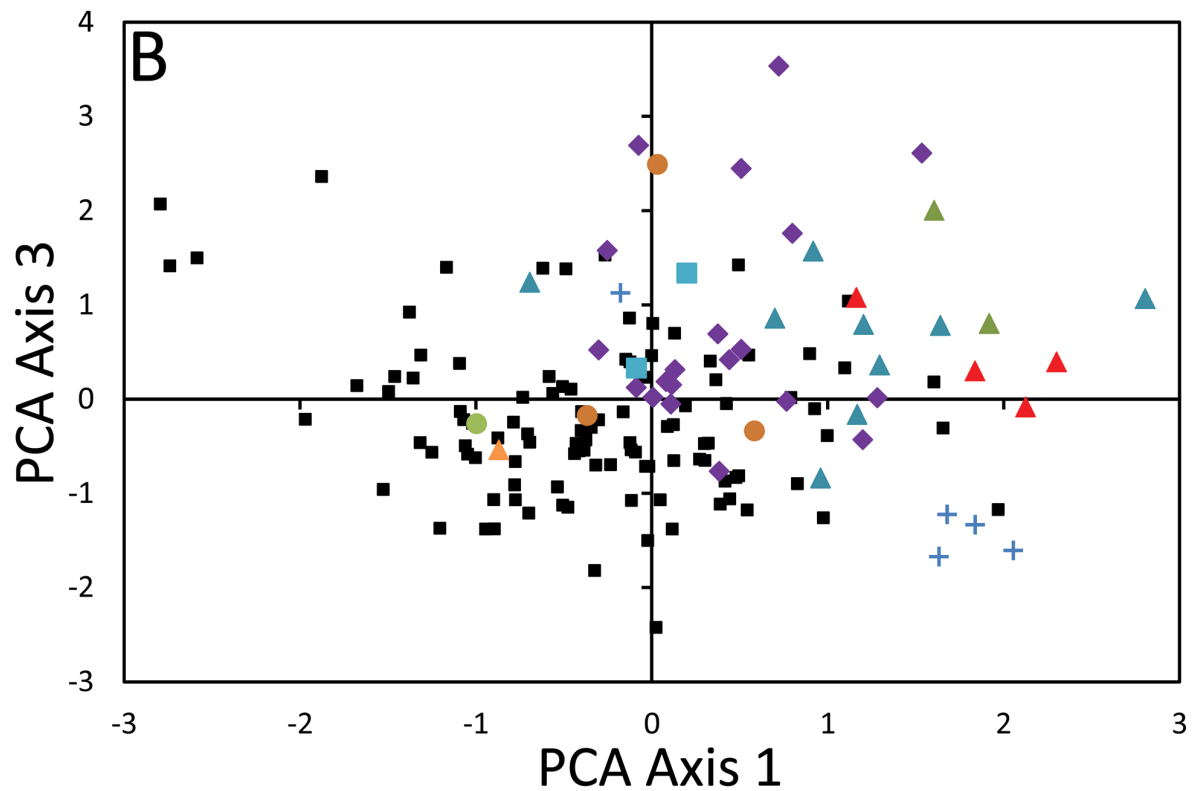
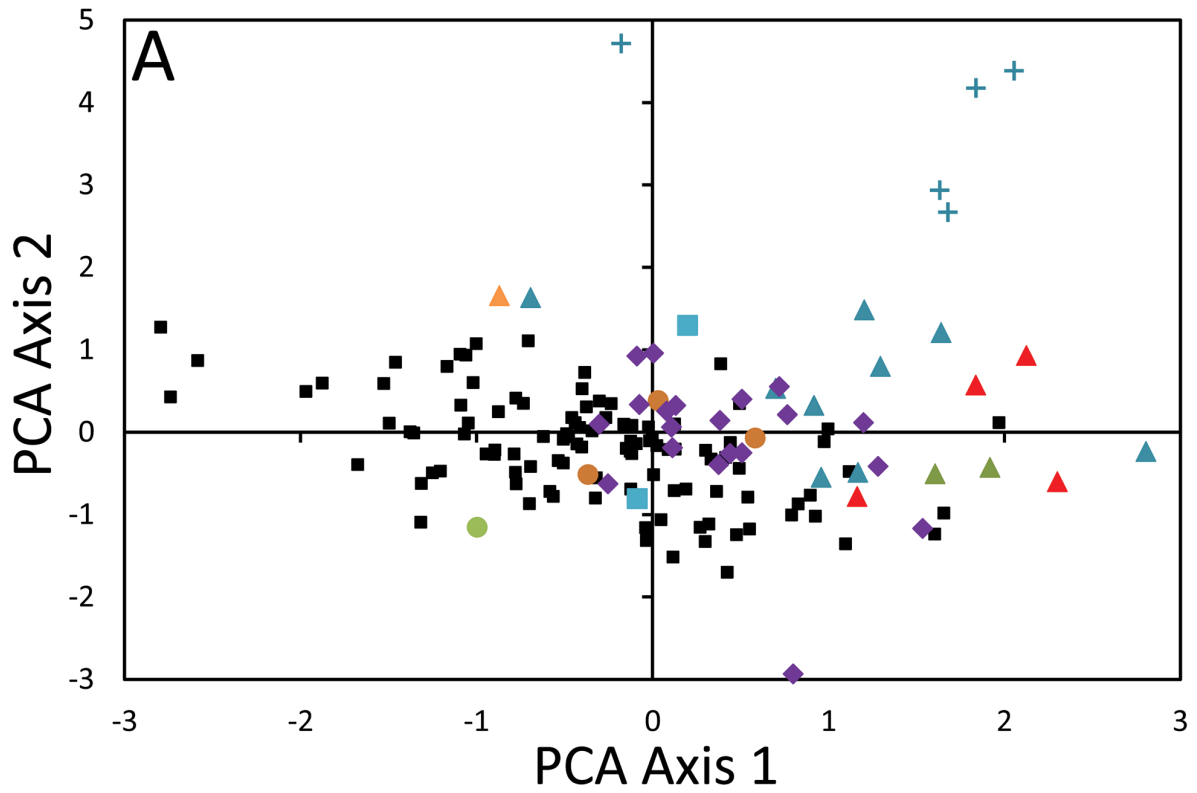
FIGURE 8. Procrustes superposition of landmarks and corrected semilandmarks. (A) all 152 *Acesta* specimens, and (B) 105 specimens of *Acesta excavata*.

Principal Component Analysis (PCA). The scatter plots of PCA scores with species identification coding highlights differences in shapes between specimens (Fig. 9). The first four components of the PCA for all 152 specimens explained 28.3%, 25.3%, 22.2% and 7.2% of the dataset variation, respectively. Only the first three components are examined here as they alone explain 75.7% of the total variance in the dataset.

PCA scores along components 1 and 2 (Fig. 9A) reveal a clear separation of *Acesta oophaga*, primarily along the principal component (PC axis) 2. This is explained to a high degree by *A. oophaga*'s distinctive lunule; its actual deformation can be seen on the thin-plate spline deformation grid of Figure 10D showing a distinctive curving of the lunule towards the center of the shell. At the opposite (negative) end of PC axis 2, only one of *A. rathbuni* stands out of the main cluster of points. Most specimens from Newfoundland and Nova Scotia, along with the two Azores specimens, are located outside the bulk of the *A. excavata* cluster of points, towards the positive end of the PC axis 1 (Fig. 9A). *Acesta bullisi* and *A. rathbuni* are mostly found within the main cluster of points, which is primarily made up by *A. excavata*.

Figure 9B shows that *Acesta oophaga* does not separate as much from the rest of the species along PC axis 3, but still has four points in the lower right quadrant of the diagram that separate along PC axis 1; the fifth *A. oophaga* specimen is found to the upper left portion of Figure 9B, on the margin of the main cluster of *A. excavata* points. Many of the specimens of *A. rathbuni* are found in the upper (positive) portion of PC axis 3.

Thin-plate spline deformation grids from PCA. The thin-plate spline deformation grids (Fig. 10) illustrate the main differences in shell shape between specimens found toward the extremities of the first three principal components, relative to the reference specimen (i.e., the Procrustes average of all specimen shapes). The deformation grid at the negative end of PC axis 1 (Fig. 10A) represents specimens with an anteriorly shifting shell body and a posteriorly shifting hinge line/dorsal region and upper lunule. Specimens with positive PC axis 1 scores (Fig. 10B) display the mirroring pattern of posteriorly shifting shell body and anteriorly shifting hinge line/dorsal region and upper lunule, with slight narrowing of the hinge (Fig. 10B). Most specimens from Newfoundland and Nova Scotia, along with those from the Azores, are found near that end of the PCA diagram.



- | | | | | |
|------------|-----------|---------------|----------------|-----------|
| ■ excavata | ▲ Azores | ▲ Nova Scotia | ▲ Newfoundland | ● bullisi |
| + oophaga | ● goliath | ◆ rathbuni | ■ saginata | ▲ smithi |

FIGURES 9. Principal component analysis of Procrustes coordinates for all 152 *Acesta* specimens. (A) axis 1 vs. axis 2. (B) axis 1 vs. axis 3.

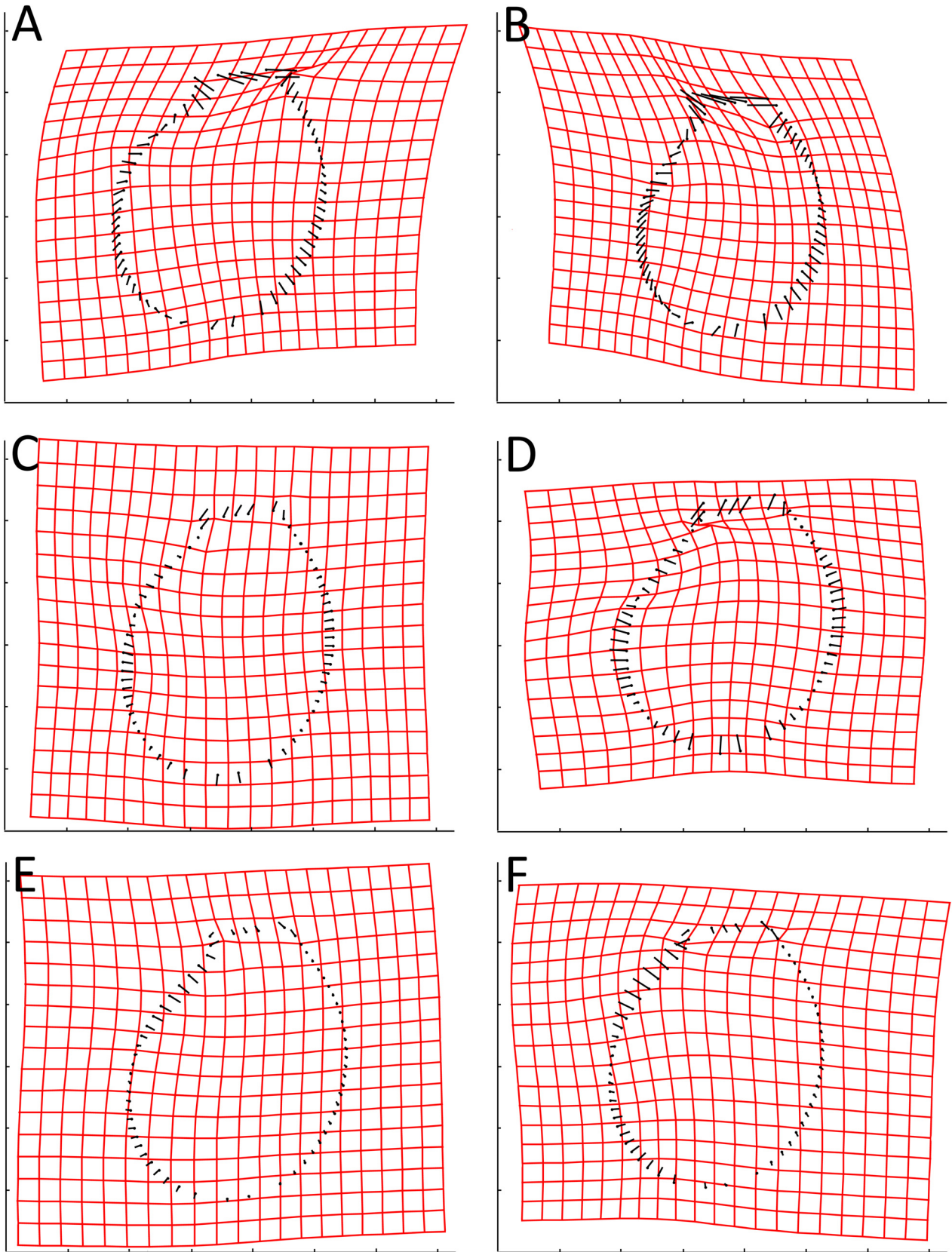


FIGURE 10. Thin-plate spline deformation grids for the extremities of each principal component for all 152 *Acesta* specimens. (A–B) axis 1. (C–D) axis 2. (E–F) axis 3. (exaggeration factor = 1.2)

The deformation grid for specimens with negative PC axis 2 scores (Fig. 10C) displays a dorsoventral elongation accompanied by an anteroposterior narrowing of the shell body. In comparison, specimens with positive PC axis 2 scores (Fig. 10D) are anteroposteriorly broader and dorsoventrally shorter, typical of *Acesta oophaga*. The deformation grids for PC axis 3 mainly illustrate the separation of specimens with distinct, linear lunule (Fig. 10E) from rounder ones with less prominent lunule (e.g., *A. rathbuni*; Fig. 10F).

Shell variation in *Acesta excavata*. The separate principal component analysis of the 105 specimens of *Acesta excavata* from Norway and Iceland shows, for the most part, a variable but strong grouping of specimens not illustrated here but similar to the one seen in Figure 9. There are, at most, nine specimens that stand out from the main cluster of points along the first three PCA axes. These tend to represent extremes in shell shape variation, often related to the length and width of the shell (e.g., rounder vs. narrower) and the hinge length. An examination of each of these shells does not suggest that they are particularly aberrant in shape; therefore, they are not considered outliers and are included in all analyses to represent the full variation in shape of *A. excavata*. One of the two Icelandic specimens is found amongst these nine ‘extremes’ while the other one falls in the middle of the *A. excavata* cluster. If the two specimens from the Azores had been included with all other *A. excavata*, they would both have fallen outside the main *A. excavata* cluster, not too far from the first (‘extreme’) Icelandic specimen (see Fig. 9A; *A. excavata* point above the two Azorean specimens). Most of the remaining specimens showing ‘extreme’ shell shape are from Norwegian fjords.

Canonical Variates Analysis (CVA). The CVA was performed on the Procrustes coordinates after a PCA reduction. The resulting first axis identifies *Acesta oophaga* (Fig. 11A, blue crosses) as the most distinct group, away from all other specimens. Most Newfoundland and Nova Scotia specimens are close to, but mostly separated from the *A. excavata* group, particularly along the first two CVA axes. *Acesta rathbuni* lies mostly between the Newfoundland and Nova Scotia group and the *A. excavata* group along CVA axis 2 while along CVA axis 3, they plot mostly below the *A. excavata* cluster, away from most Newfoundland and Nova Scotia specimens.

The jackknife test resulted in 0.1% of the specimens correctly classified and significant, 46.6% being correctly classified and non-significant, 0.2% being incorrectly classified and significant, and 53.0% being incorrectly classified and non-significant. These results suggest there is no significance in the assignment of specimens within existing groupings and that those assigned correctly (46.7%) can just as easily be assigned to the correct groupings by chance alone. When Newfoundland and Nova Scotia specimens are treated as unknowns in the CVA (not illustrated here), the resulting distribution along the first three axes is similar to that observed in Figure 11, although these tend to aggregate more with *Acesta excavata*. With such weak discrimination between groups, the deformation grids (not illustrated) display little consistent information, except for the one representing the *A. oophaga* shape.

Genetic analyses. The aligned partial COI gene sequence dataset comprises 589 nucleotides; three nucleotide gaps were inserted into the *Acesta* sequences to align them with species of *Lima* and *Limaria*. The 61 *Acesta* sequences were identical at 432 of 586 bases (74%) with no deletions or insertions in the multiple sequence alignment. Intraspecific variation was low (*A. bullisi* 0.68%; *A. oophaga* 0.85%; *A. excavata* 0.68%; *A. sphoni* 0.52%; *A. mori* (Hertlein, 1952) 6.83%; five specimens of *Acesta* from the northwest Atlantic 2.90%). Average within group MCL distances was correspondingly low (*Limaria* 0.282; *A. bullisi* 0.005; *A. oophaga* 0.004; *A. excavata* 0.004; *A. sphoni* 0.003; *A. mori* 0.005; five specimens of *Acesta* from the northwest Atlantic 0.012). Genetic divergence between sequence pairs within *Acesta* species, including the Newfoundland and Nova Scotian samples as a group, was an order of magnitude greater and ranged from 0.047 (*A. oophaga* and *A. mori*) to 0.166 (*A. sphoni* and *Acesta* from Newfoundland and Nova Scotia) (Tab. 7). In contrast, the average MCL distance between the genera *Limaria* and *Acesta* ranged from 0.606 to 0.649 (Tab. 7).

The inferred evolutionary tree with the highest log likelihood (-3666.98) is shown in Figure 12. The analysis involves 64 nucleotide sequences. All five *Acesta* species are well resolved and the specimens from The Gully and Beothuk Knoll (Tab. 3) form a distinct clade. The MP consensus tree inferred from the 66 most parsimonious trees is shown in Figure 13, with branches corresponding to partitions reproduced in less than 50% of the trees being collapsed. The relative amount of homoplasy was high with a consistency index of 0.72 (0.69) and a retention index of 0.85 (0.85) for all sites and parsimony-informative sites (in parentheses). The percentage of parsimonious trees in which the associated taxa clustered together is shown next to the branches. All species formed well-supported clusters with 100% of the MP trees supporting the configuration. As for the ML tree, the five *Acesta* specimens from the northwest Atlantic formed a distinct clade.

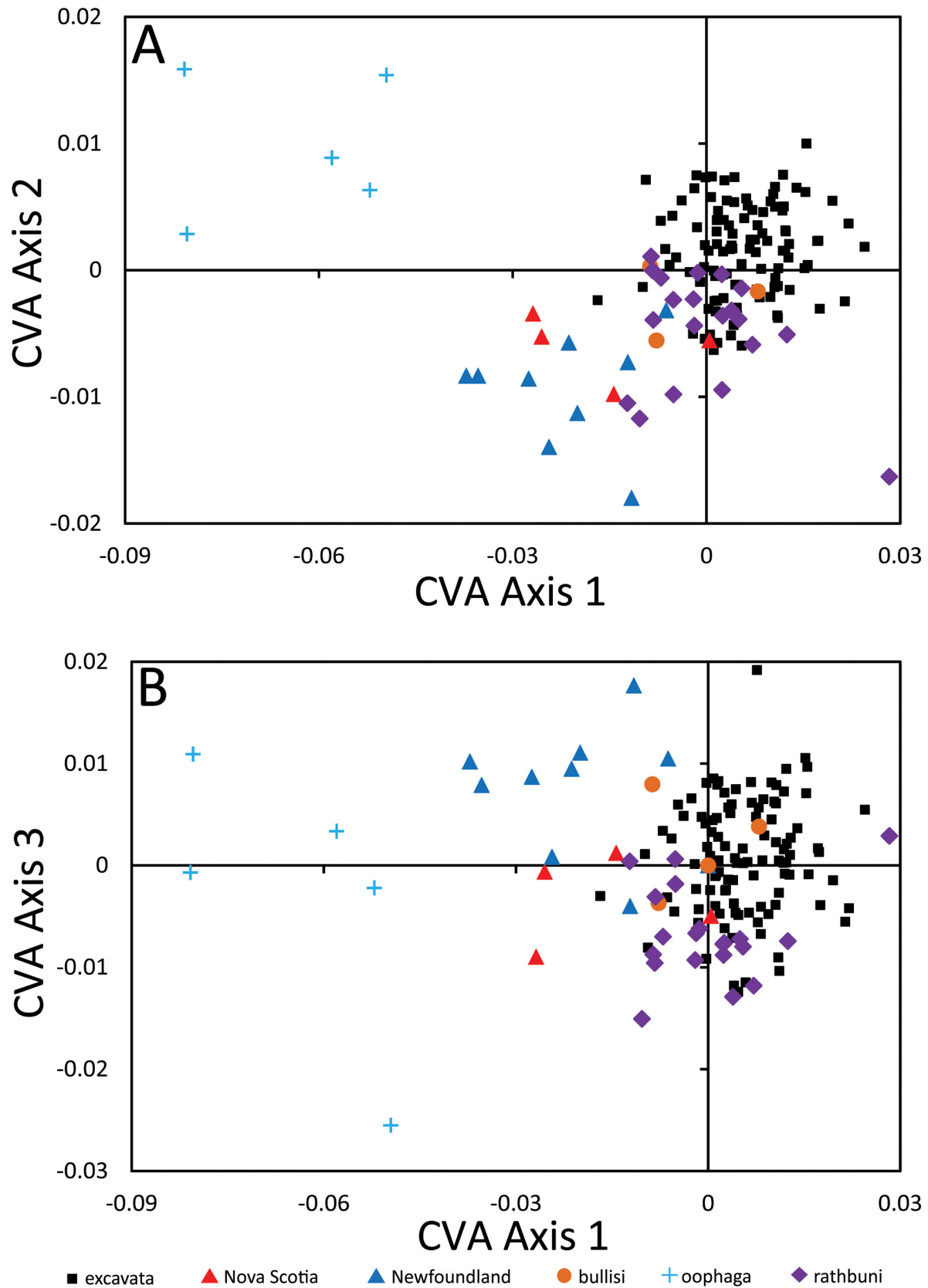


FIGURE 11. Canonical variate analysis of the Procrustes coordinates for all *Acesta* groups (146 specimens) with at least three specimens, based on a PCA reduction to 10 axes. (A) axis 1 (eigenvalue = 3.096) vs. axis 2 (eigenvalue = 0.983). (B) axis 1 vs. axis 3 (eigenvalue = 0.347).

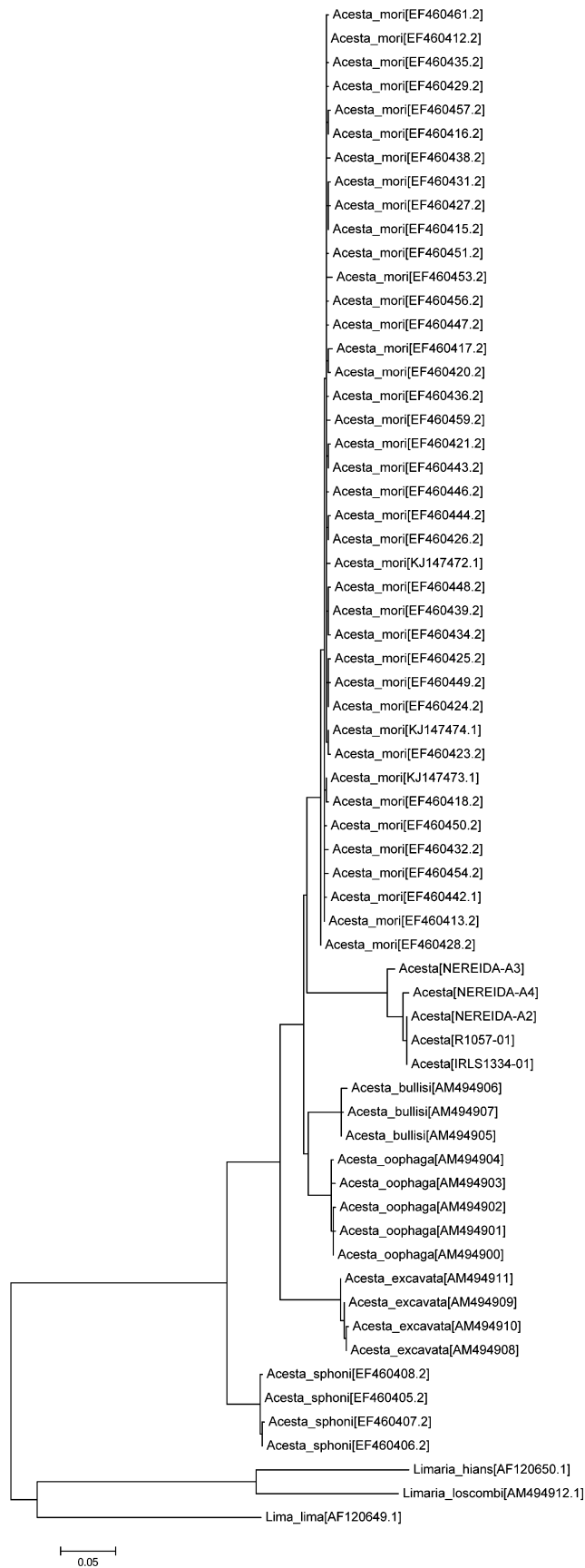


FIGURE 12. Molecular phylogenetic analysis of *Acesta*, *Lima* and *Limaria* species by Maximum Likelihood method based on partial COI gene sequences (589 bp). The tree is drawn to scale, with branch lengths measured in the number of substitutions per site.

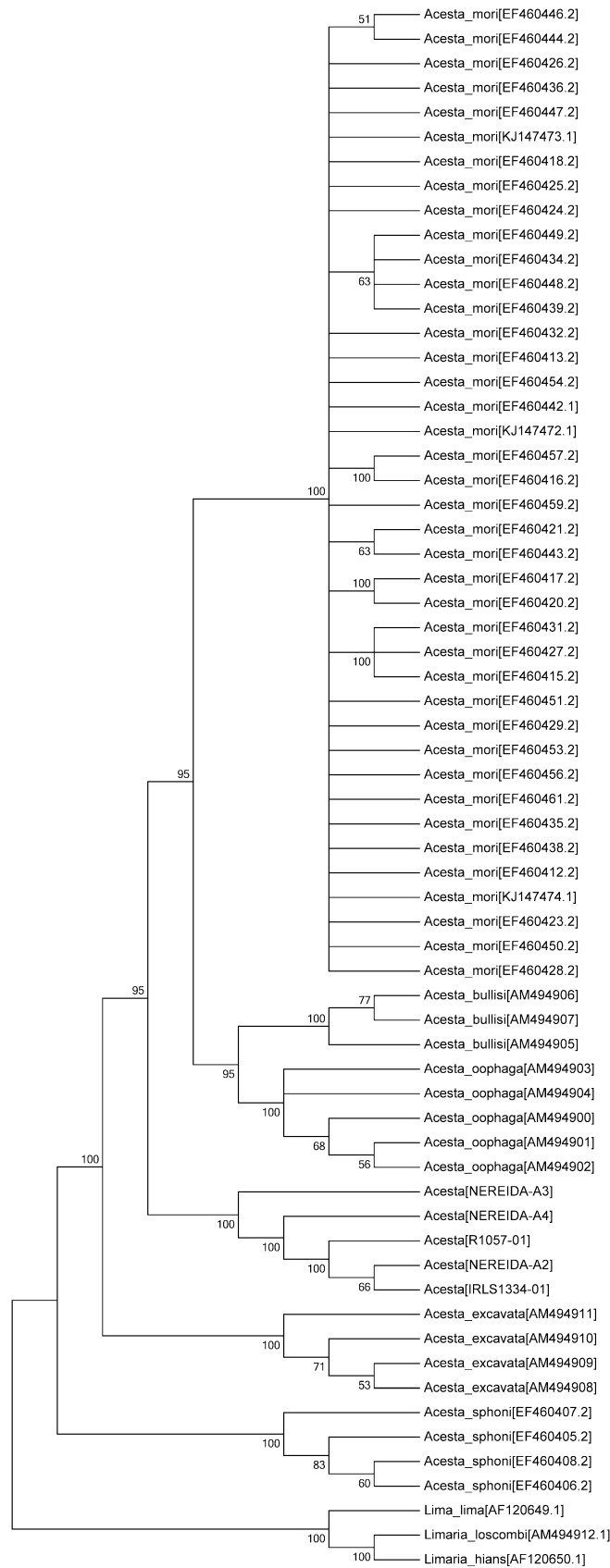


FIGURE 13. Maximum parsimony consensus tree of *Acesta* taxa inferred from 66 most parsimonious trees. Branches corresponding to partitions reproduced in less than 50% trees are collapsed. The percentage of parsimonious trees in which the associated taxa clustered together is shown next to the branches. The root was placed on the branch leading to *Lima lima* (Linnaeus, 1758) and the *Limaria* Link, 1807, species.

Collectively, the phylogenetic analyses indicate species status for the *Acesta* specimens from the northwest Atlantic. These specimens group together, using comparative evolutionary trees, have similar levels of intraspecific variation and form branch lengths similar to those resolving other *Acesta* species.

TABLE 7. Estimates of evolutionary divergence over sequence pairs between groups of *Acesta* and *Limaria*. The numbers of base substitutions per site calculated by averaging over all sequence pairs between groups using the Maximum Composite Likelihood method (following Tamura *et al.* 2004) are shown.

	<i>Limaria</i>	<i>A. sphoni</i>	<i>Acesta</i> NL+NS*	<i>A. excavata</i>	<i>A. bullisi</i>	<i>A. oophaga</i>
<i>A. sphoni</i>	0.606					
<i>Acesta</i> NL+NS*	0.649	0.166				
<i>A. excavata</i>	0.624	0.136	0.142			
<i>A. bullisi</i>	0.609	0.118	0.113	0.106		
<i>A. oophaga</i>	0.607	0.117	0.119	0.101	0.052	
<i>A. mori</i>	0.612	0.117	0.103	0.092	0.055	0.047

* *Acesta* specimens from Newfoundland & Nova Scotia, NW Atlantic (*A. cryptadelphe* sp. nov.).

Discussion

This study represents the first quantitative examination of the shell shape for species belonging to the genus *Acesta*, with particular emphasis on groups found in the North Atlantic. For this genus, the use of external shell features is mainly limited to the presence or absence of radial ribs, as well as their specific form over different regions of the shell. López Correa *et al.* (2005) provide a description of this character for *A. excavata*, which is confirmed by our observations, along with a fair degree of intraspecific variation. This character, however, does not appear to distinguish Newfoundland and Nova Scotia specimens from the European giant file clam, as observed by Gagnon & Haedrich (2003) for the Bay d'Espoir specimens. This is also the case for specimens from the Azores and even for *A. bullisi* (Gulf of Mexico) and *A. saginata* (southwest Pacific–New Zealand), which show radial rib patterns very similar to those of *A. excavata*.

A few studies have compared traditional morphological measurements and associated ratios between species. Boss (1965) compared shell height, width and inflation, along with ratios, between *Acesta excavata* and *A. angolensis* (Adam & Knudsen, 1955) and found greater lateral expansion (i.e., shell inflation) in the former species. Marshall (2001) compared shell length and width, hinge length and single valve inflation for three *Acesta* species from the southwestern Pacific, including *A. saginata*, but did not compare them to *A. excavata*. Gagnon & Haedrich (2003) examined the shell height/width ratio and found no significant difference between the first two Newfoundland specimens recovered and *A. excavata*. The morphological measurements and ratios obtained in this study generally show a fair amount of overlap between species, particularly when characters such as shell width, hinge length and valve inflation are compared to shell length (Fig. 7). Some species, such as *A. oophaga* and *A. rathbuni* do show some differences for these morphological characters, but rarely to a point where they can be fully differentiated from *A. excavata*. The midline-width-ratio is the one morphological character that shows a significant difference in shell proportion between the *A. excavata* group from Norway and Iceland and the Newfoundland, Nova Scotia, and probably the Azores specimens (Tab. 6, Fig. 7F). These specimens, along with those of *A. oophaga* and *A. rathbuni*, have a proportionally smaller anterior region of the shell in relation to the position of the perpendicular line from LM-1 (Fig. 5). The shell shape analysis also demonstrates overlap between species. The key observation is that *Acesta excavata* shows a wide variability in shape (Fig. 9) with small specimens showing less variation (Fig. 7A–E). However, the causes are not analysed here. The analyzed specimens of *A. bullisi* and *A. rathbuni* display less variability in shell shape but still fall within the cluster of points formed by *A. excavata*. Of course, this observation may be the result of small sample size.

Specimens from off Newfoundland (including those from Bay d'Espoir) and Nova Scotia fall on the edge of *Acesta excavata* shape variability (Fig. 9). It is likely that this pattern reflects, at least in part, the above-mentioned difference observed for the midline-width-ratio, i.e., the posterior prominence of the shell (Tab. 6, Fig. 7F). Similarly, the two specimens from the Azores seem to be distinct from *A. excavata*, although the sample size is

very small. If the few ‘extreme’ *A. excavata* variants are removed from the analysis (not illustrated here), the result shows hardly any overlap with the mid- and northwest Atlantic groups; but there is still no full separation from *A. excavata* as compared to *A. oophaga*.

The thin-plate spline deformation grids illustrate differences in the shape of the hinge. Most of the specimens from Newfoundland, Nova Scotia and the Azores show an anterior shift and narrowing (particularly the anterior portion) of the hinge accompanied with a posterior shift of the shell body (Fig. 10B). Vokes (1963) also observed a relatively short hinge line for *A. bullisi*, probably referring to specimens of both Gulf of Mexico species (Tab. 6). Although the CVA shows clustering of *A. oophaga* away from the other points and of the Newfoundland and Nova Scotian specimens near the *A. excavata* group, the results are not statistically significant in terms of group assignment. The jackknife assignment test confirms that the shape variation within *A. excavata* and between the latter and the Newfoundland and Nova Scotian specimens is too great to obtain a clear discrimination of these groups.

The shell shape of *Acesta* specimens from the Mid-Atlantic Ridge (north of the Azores) appears to fall outside the range of variability displayed by the typical Norwegian *A. excavata*, suggesting the former may also be a distinct species. However, further genetic analyses of mid-Atlantic specimens are required to test this possibility.

Results of the adult shell shape analysis and examination of external shell characters, in and of themselves, do not provide a reliable means to separate the *Acesta* groups in the North Atlantic Ocean, with the exception of *A. oophaga*. The limited information on larval shell size obtained in this study, however, suggests that the northwest Atlantic specimens can be distinguished from the Norwegian specimens of *A. excavata*. The value of 217 µm reported by Järnegren *et al.* (2007) for *A. excavata* falls closer to the range observed here for Norwegian specimens than to that of the northwest Atlantic specimens. Although the observed difference in range is not statistically conclusive, it is consistent with the differentiation of a new species based on genetic data (see below). Further observations, preferably using a SEM (for better resolution and greater precision in measurement) and with a greater sample size, are necessary to test this difference in larval shell size, however.

The molecular data based on COI gene sequences show that the northwest Atlantic specimens and the other species analysed here diverge by 7%. This is twice the genetic divergence between *A. oophaga* and *A. bullisi*, suggesting that the northwest Atlantic specimens represent a distinct cryptic species, which we call *A. cryptadelphe* **sp. nov.**

The two consensus methods (Figs. 12, 13) cluster specimens of *Acesta cryptadelphe* **sp. nov.** more closely with *A. bullisi* and *A. oophaga* from the Gulf of Mexico, and *A. mori* from the northeast Pacific, suggesting a more recent affinity than with *A. excavata*. Furthermore, *A. mori* (Hertlein, 1952) (Clague *et al.* 2012) appears to be morphologically and genetically closer to the North Atlantic “*excavata*” group than to *A. sphoni*, its northeast Pacific sibling, which is morphologically more similar to *A. smithi*, a southwestern Pacific species included in the subgenus *Plicacesta* by Hertlein (1963) and Vokes (1963). Here as well, further genetic studies may help resolve the evolutionary origin of these species within the Atlantic and Pacific Oceans.

Systematics

Class BIVALVIA Linnaeus, 1758

Subclass PTERIOMORPHIA Beurlen, 1944

Order LIMOIDA Moore, 1952

Superfamily LIMOIDEA Rafinesque, 1815

Family LIMIDAE Rafinesque, 1815

Genus *Acesta* H. & A. Adams, 1858

***Acesta cryptadelphe* sp. nov.**

Figs. 2, 3C–D, 6, 14–16

Material examined. Collection data for each sample set is shown in Table 2. The holotype and three paratypes are from The Gully, off Nova Scotia; nine paratypes are from Beothuk Knoll, off northeast Newfoundland (southwest Flemish Cap), including the tissue from two specimens separated from their respective shell; and two paratypes are from the main basin of Bay d’Espoir, southern Newfoundland (Gagnon & Haedrich 2003).

Table 3 summarizes the catalogue/accession information and basic morphological data for each specimen included in the type series. All specimens are deposited in the Mollusc Collection of the Canadian Museum of Nature; five of these were used to extract partial COI gene sequence datasets, which are available on GenBank.

Description. Holotype (CMNML 097156): Complete specimen, left valve preserved dry (Fig. 14A), right valve (posterior margin damaged) and tissue preserved in 70% ethanol; nearly equivalved (see byssal notch below), thin, ovate with narrow hinge region (hinge length to shell width ratio = 0.43; Tab. 3), exterior light beige in colour, with whitish radial ribs in median portion of shell; anterior and posterior radial ribs most prominent, attenuating toward median region, becoming broader and flattened; at least 8–9 major growth lines irregularly interrupting radial ribs. Poorly developed anterior auricle, dorsally delineating lunule; posterior auricle extending from umbo and representing about 83% of hinge length (Tab. 3). Lunule length 3.5 cm, representing 41% of shell length, with weak inward curve. Byssal notch indistinct on left valve with lunule inner margin nearly straight, slightly gapping on right valve, particularly toward the dorsal region of the lunule. Shell moderately inflated with highest inflation point at first third of shell length.

Shell interior translucent, glossy, whitish, with weak but demarcated muscle scars in the dorsoposterior region of the shell; pallial line weak. Hinge plate with deep, oblique, V-shape ligament pit extending from shell beak to mid-ventral edge of hinge plate. Hinge line delineating interior edge of hinge plate on either sides of ligament pit, nearly linear; ligament pit extending only slightly ventrally below hinge line; hinge length approx. 32% of shell length; hinge plate approx. 0.5 cm high from beak to hinge line (about 5.2 % of shell length). Umbonal cavity present behind hinge plate.

Soft tissue: mantle margin uniform and unfused, without siphon, bordered by short (contracted) tentacles. Foot small with broad, distal sole with deep byssal groove; three byssal threads attached anterodorsally to base of foot. Mouth bordered above and below by short palps, forming wide “lips”; palps not connected to gills. In living animal, soft tissue bright orange in colour, with long tentacles extending from gaping mantle margin (Fig. 2).

Character variations within type series: Tables 3 and 6 and Figure 7 present some of the morphometric variations between specimens. Shell thin, almost transparent in smallest specimen (CMNML 097162, Fig. 15), whitish to beige, translucent in some intermediate specimens (CMNML 097158, Fig. 3D; CMNML 097157.1, Fig. 14B) and thick, opaque with patchy whitish, beige to light brown exterior and white interior in oldest specimens (e.g., CMNML 092958, CMNML 097161.1); highest valve inflation point closer to middle of shell length in larger specimens (valve inflation to shell length ratio ranges from 0.15 to 0.26; Fig. 7E), shell width to length ratio ranges from 0.74 to 0.84. Lunule of variable length relative to shell length with ratios ranging from 0.22 to 0.58 (Fig. 7C). Byssal notch usually represented by slight gapping of right valve, occasionally on both valves (e.g., CMNML 097157.1). Hinge length to shell length ratio ranges from 0.24 to 0.32; hinge plate height to shell length ratio varies from 0.031 in smallest specimens (e.g., Figs. 14B, 15B) to 0.102 in older specimens (e.g., Fig. 16B, D); hinge length to shell-width-ratio ranges from 0.30 to 0.43. Prominence of radial ribs on exterior of valves variable, faint in some specimens (e.g., CMNML 097160.2, CMNML 097161.1).

The two specimens with well-preserved larval shell from The Gully and Beothuk Knoll (Tab. 5; Fig. 6) display a dome-shaped, subcircular prodissoconch (P1), with a uniform glossy surface; shell type 2D (or 2C?) (Malchus & Sartori 2013). Their lengths vary between 241 and 261 μm . A prodissoconch 2 region could not be clearly identified by light microscopy.

Distribution. Only known from the material examined, off Nova Scotia, in The Gully, from 619 to 1241 m, and around Beothuk Knoll, southwest Flemish Cap, from 710 to 888 m, and from Newfoundland in Bay d’Espoir’s Main Basin, from approx. 400 to 785 m. See Figure 1 for map.

Etymology. From the terms “crypto”, meaning hidden or concealed, and “adelphe”, meaning sister or sibling, referring to the very similar shell morphology between this northwest Atlantic species and *Acesta excavata* in the northeast Atlantic.

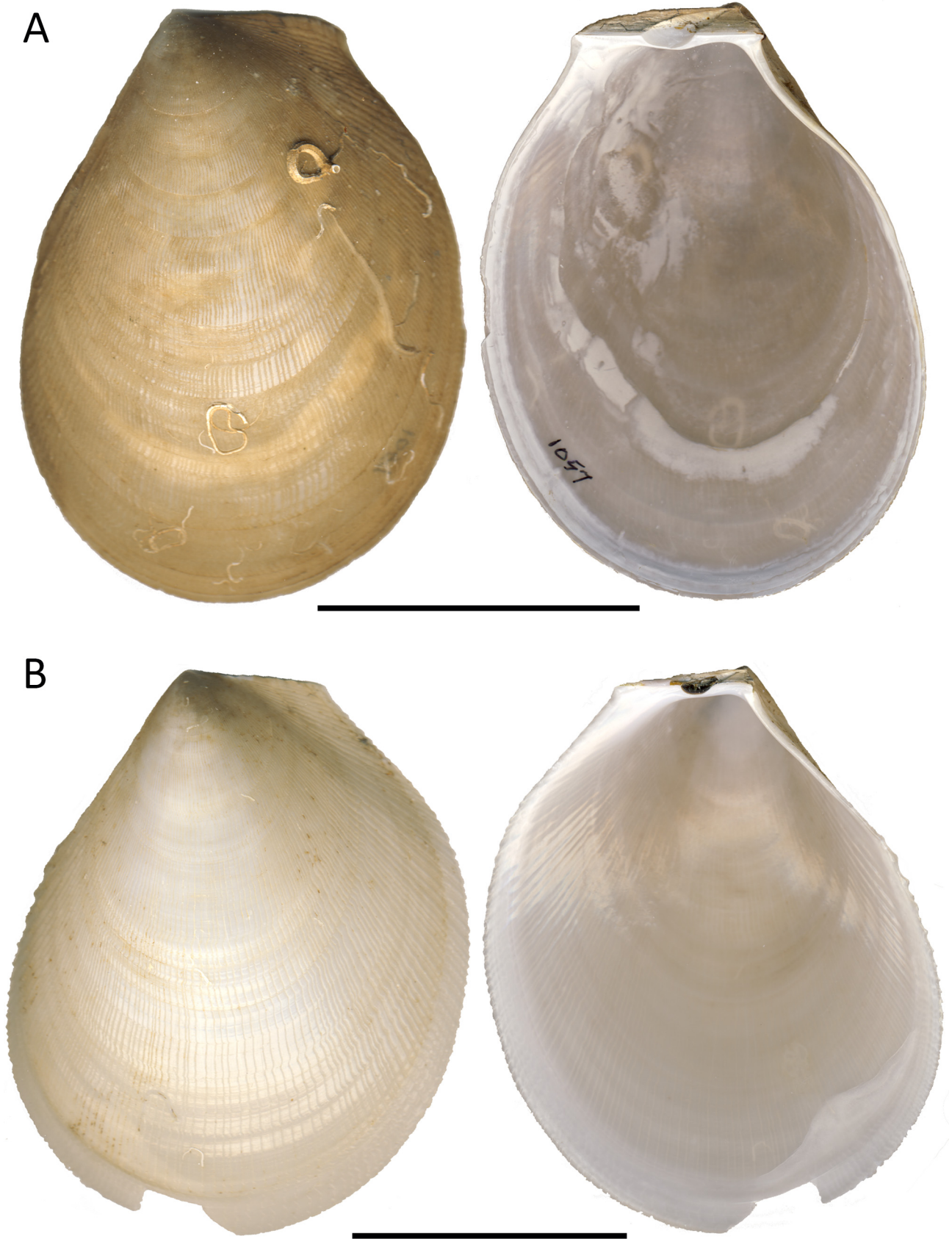


FIGURE 14. External and internal views of the valves of *Acesta cryptadelphe* sp. nov. from The Gully, offshore Nova Scotia. (A) Holotype CMNML 097156, left valve. (B) Paratype CMNML 097157.1, left valve. Scales = 5 cm.



FIGURE 15. External and internal views of the valves of *Acesta cryptadelphe* **sp. nov.** from Beothuk Knoll, southwest Flemish Cap. (A) Paratype CMNML 097159.1, left valve; scale = 5 cm. (B) CMNML 097162, left valve; scale = 0.2 cm.

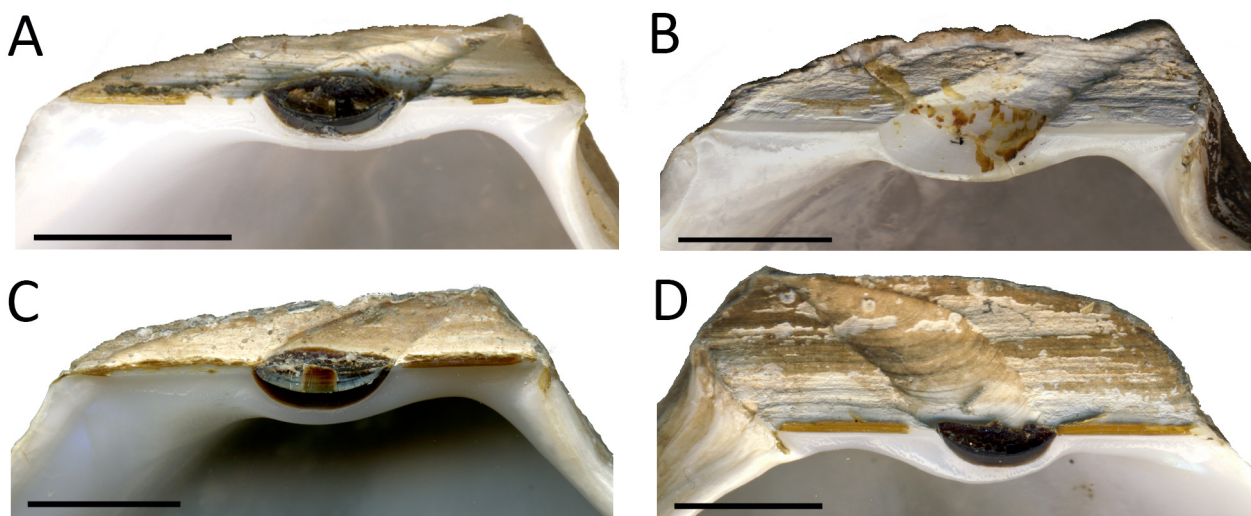


FIGURE 16. Close-up internal view of the hinge of *Acesta cryptadelphe* **sp. nov.** from The Gully (offshore Nova Scotia), Bay d'Espoir (Newfoundland), and Beothuk Knoll (southwest Flemish Cap). (A) Paratype CMNML 097157.2, left valve; The Gully. (B) Paratype CMNML 092958, left valve; Bay d'Espoir. (C) Paratype CMNML 097160.1, left valve; Beothuk Knoll. (D) Paratype CMNML 097159.2, right valve; Beothuk Knoll. Scales = 1 cm.

Remarks. There is no DNA information available for the specimens collected by Gagnon & Haedrich (2003) in Bay d'Espoir, Newfoundland. However, according to our shell shape analysis, the specimens cluster with the Beothuk Knoll and The Gully specimens, which plot marginally outside the *Acesta excavata* cluster suggesting that they share close genetic affinities. The specimens from the Azores also cluster along with the Newfoundland and Nova Scotia specimens in the shell shape analysis, and may also represent *A. cryptadelphe* **sp. nov.** Further genetic work on Azorean specimens is required to test that hypothesis.

The molecular data indicate that the *Acesta* species, including *A. cryptadelphe* **sp. nov.**, each form a monophyletic clade (Figs. 12, 13). The specimens from Newfoundland (Beothuk Knoll) and Nova Scotia (The Gully) have a low genetic divergence (average 0.012) comparable to that of other *Acesta* species (range 0.003 to

0.012), and with divergence from other *Acesta* species an order of magnitude greater; ranging from 0.103 (*A. mori*) to 0.166 (*A. sphoni*).

Habitat and species association. In the northwest Atlantic (Fig. 1), all specimens were found associated with rocky substrates below 400 m water depth, either on isolated outcrops, under overhangs or on rock walls. The first two specimens of giant file clams found in Bay d'Espoir, Newfoundland, were associated with a near-vertical underwater cliff and isolated outcrops at depths ranging from 400 to 800 m (Gagnon & Haedrich 2003). A manned diving excursion with a submersible along two vertical transects of this fjord's rock walls (Goblin Head; Haedrich & Gagnon 1991) revealed large numbers of *Acesta* specimens but none of the typical cold-water coral association (i.e., *Paragorgia arborea*, *Primnoa resedaeformis*, *Lophelia pertusa* and *Madrepora oculata* (Linnaeus), *Desmophyllum* Ehrenberg. In The Gully, *Acesta* specimens occur on steep cliffs and other rock surfaces, in association with *Desmophyllum dianthus* (Esper) (Fig. 2B), *Paramuricea* Koelliker, and occasionally in the vicinity of *Primnoa resedaeformis* (Gunnerus) (Kenchington *et al.* 2014). Around Beothuk Knoll, Murillo *et al.* (2011) reported *Paragorgia arborea* and *Desmophyllum dianthus* whereas *Primnoa resedaeformis* and *Anthothela grandiflora* (M. Sars) are present within Flemish Pass, just north of Beothuk Knoll.

Acknowledgements

We thank the following individuals and affiliated institutions for providing access to collection specimens, through loans or by providing images of the whole shell: Ole S. Tendal and Martin Vinther Sørensen of the Zoological Museum, University of Copenhagen, Denmark; Manuel Malaquias and Katrine Kongshavn at the Norwegian University of Life-sciences, Bergen, Norway; Yves Barette of the Institut royal des Sciences naturelles de Belgique, Brussels, Belgium; Ellen Strong of the Smithsonian National Museum of Natural History, Washington, USA; and Mark Siddall & Christine Lebeau of the American Museum of Natural History, New York, USA. Additional thanks are due to Martin Vinther Sørensen and Katrine Kongshavn who also provided images of the larval shell for specimens from Norwegian fjords. We are also grateful for the generous efforts of several volunteers who helped in processing images: Vesta Mather, Ben Angel and François Bregha; shell images from AMNH and USNM were obtained by Vesta Mather. All the Beothuk Knoll specimens were provided by the Spanish Institute of Oceanography, Vigo, Spain, via F. Javier Murillo; they were collected as part of the NAFO Potential Vulnerable Marine Ecosystems-Impacts of Deep-Sea Fisheries project (NEREIDA), which is supported by Spain's General Secretary of the Sea (SGM), Spain's Ministry for the Rural and Marine Environment, the Spanish Institute of Oceanography, the Geological Survey of Canada, the Canadian Hydrographic Service, Fisheries and Oceans Canada, the UK's Centre for the Environment Fisheries and Aquaculture Science (Cefas), the Russian Polar Research Institute of Marine Fisheries and Oceanography, and the Russian P.P. Shirshov Institute of Oceanology (RAS). The authors would like to acknowledge the hard work of the crew and scientist staff on board the research vessels *Miguel Oliver* and *CCGS Hudson* (and ROPOS) that collected the samples for this study. We appreciate the valuable advice provided by H. David Sheets for the shell shape analysis and by André Martel for the examination of larval shells. We thank Tyler Jordan and Lindsay Beazley of the Bedford Institute of Oceanography for their expert assistance with DNA extraction and data mining, respectively. Finally, we are most grateful for the critical reviews of the manuscript provided by Jon-Arne Snøli and the editor.

References

- Adam, W. & Knudsen, J. (1955) Note sur quelques espèces de mollusques marins nouveaux ou peu connus de l'Afrique Occidentale. *Mededelingen Koninklijk Belgisch Instituut voor Natuurwetenschappen*, 31 (61), 1–25.
- Bartsch, P. (1913) The giant species of the molluscan genus *Lima* obtained in the Philippine and adjacent waters. *Proceedings of the U.S. National Museum*, 45, 235–240.
- Bookstein, F. (1997) Landmark methods for forms without landmarks: morphometrics of group differences in outline shape. *Medical Image Analysis*, 1, 225–243.
[http://dx.doi.org/10.1016/S1361-8415\(97\)85012-8](http://dx.doi.org/10.1016/S1361-8415(97)85012-8)
- Boss, K. (1965) Note on *Lima (Acesta) angolensis*. *Nautilus*, 79, 54–58.
- Bruguère, J.G. (1797) *Tableau encyclopédique et méthodique des trois règnes de la nature. Contenant l'helminthologie, ou les vers infusoires, les vers intestins, les vers mollusques, etc. Troisième livraison*, Panckoucke, Paris, 97 pls. [pls. 190–286]

- Brusoni, F. & Basso, D. (2007) Canonical morphometry versus statistical treatment of outlines through Fourier shape analysis: an empirical comparison. *Bollettino Malacologico*, 43, 131–138. Available from: [http://www.societaitalianadimalacologia.it/Bollettino/Volume-43/Abstract43\(9-12\)%20131-138.pdf](http://www.societaitalianadimalacologia.it/Bollettino/Volume-43/Abstract43(9-12)%20131-138.pdf) (Accesses 25 Aug. 2015)
- Clague, G.E., Jones, W.J., Paduan, J.B., Clague, D.A. & Vrijenhoek, R.C. (2012) Phylogeography of *Acesta* clams from submarine seamounts and escarpments along the western margin of North America. *Marine Ecology*, 33, 75–87. <http://dx.doi.org/10.1111/j.1439-0485.2011.00458.x>
- Copley, J.T.P., Tyler, P.A., Sheader, M., Murton, B.J. & German, C.R. (1996) Megafauna from sublittoral to abyssal depths along the Mid-Atlantic Ridge south of Iceland. *Oceanologica Acta*, 19, 549–559. <http://archimer.ifremer.fr/doc/00096/20725/> (accessed 10 August 2015)
- Dautzenberg, P. (1927) Mollusques provenant des campagnes scientifiques du Prince Albert 1^{er} de Monaco dans l'Océan Atlantique et dans le Golfe de Gascogne. *Résultats des Campagnes Scientifiques du Prince Albert 1^{er} de Monaco*, 52, 1–400.
- Durán Muñoz, P., Sacau, M., Del Rio, J.L., López-Abellán, L.J. & Sarralde, R. (2014) Seabed mapping and vulnerable marine ecosystems protection on the high-seas fisheries: Four case studies on progress in the Atlantic Ocean. *ICES CM 2014/3527 B:22*. Available from: <http://www.ices.dk/sites/pub/CM%20Documents/CM-2014/Theme%20Session%20B%20contributions/B2214.pdf> (accessed 18 July 2015)
- Fabricius, J.C. (1779) *Reise nach Norwegen mit Bemerkungen aus des Naturhistorie und Oekonomie*. Verlag Carl Ernst Bohn, Hamburg, 398 pp.
- Folmer, O., Black, M., Hoeh, W., Lutz, R. & Vrijenhoek, R. (1994) DNA primers for amplification of mitochondrial cytochrome c oxidase subunit I from diverse metazoan invertebrates. *Molecular Marine Biology and Biotechnology*, 3, 294–299. Available from: http://www.mbari.org/staff/vrijen/PDFS/Folmer_94MMBB.pdf (accessed 10 August 2015)
- Gagnon, J.-M. & Haedrich, R.L. (2003) First record of the European giant file clam, *Acesta excavata* (Bivalvia: Pectinoidea: Limidae), in the northwest Atlantic. *The Canadian Field-Naturalist*, 117, 440–447. Available from: <http://canadianfieldnaturalist.ca/index.php/cfn/article/viewFile/748/748> (accessed 10 August 2015)
- Gmelin, J.F. (1791) *Caroli a Linné, systema naturae. Tom. I. Pars VI*. Beer, Lipsiae, 890 [pp. 3021–3910]
- Goldstein, P.Z. & DeSalle, R. (2011) Integrating DNA barcode data and taxonomic practice: Determination, discovery and description. *BioEssays*, 33, 135–147. <http://dx.doi.org/10.1002/bies.201000036>
- Haedrich, R.L. & Gagnon, J.-M. (1991) Rock wall fauna of Newfoundland Fjords. *Continental Shelf Research*, 11, 1199–1208. [http://dx.doi.org/10.1016/0278-4343\(91\)90097-P](http://dx.doi.org/10.1016/0278-4343(91)90097-P)
- Hammer, Ø. (2014) *PAST–Paleontological Statistics. Version 3.05. Reference Manual*. Natural History Museum, University of Oslo, 222 pp. Available from: <http://folk.uio.no/ohammer/past/> (accessed 23 June 2015)
- Hebert, P.D.N. & Gregory, T.R. (2005) The promise of DNA barcoding for taxonomy. *Systematic Biology*, 54, 852–859. <http://dx.doi.org/10.1080/10635150500354886>
- Hebert, P.D.N., Cywinska, A., Ball, S.L. & deWaard, J.R. (2003) Biological identifications through DNA barcodes. *Proceedings of the Royal Society Series B–Biological Sciences*, 270, 313–321. <http://dx.doi.org/10.1098/rspb.2002.2218>
- Hertlein, L.G. (1952) Description of a new pelecypod of the genus *Lima* from deep water off central California. *Proceedings of the California Academy of Sciences*, 27, 377–381.
- Hertlein, L.G. (1963) A new species of giant *Lima* from off southern California (Mollusca: Pelecypoda). *Occasional Papers California Academy of Sciences*, 40, 1–6.
- Jablonski, D. & Lutz, R.A. (1983) Larval ecology of marine benthic invertebrates: paleobiological implications. *Biological Review*, 58, 21–89.
- Järnregren, J. & Altin, D. (2006) Filtration and respiration of the deep living bivalve *Acesta excavata* (J.C. Fabricius, 1779) (Mollusca: Bivalvia). *Journal of Experimental Biology and Ecology*, 334, 122–129. <http://dx.doi.org/10.1016/j.jembe.2006.01.014>
- Järnregren, J., Schander, C., Sneli, J.-A., Rønningen, V. & Young, C.M. (2007) Four genes, morphology and ecology: distinguishing a new species of *Acesta* (Mollusca; Bivalvia) from the Gulf of Mexico. *Marine Biology*, 152 (1), 43–55. <http://dx.doi.org/10.1007/s00227-007-0651-y>
- Johnson, M.P., White, M., Wilson, A., Würzberg, L., Schwabe, E., Folch, H. & Allcock, A.L. (2013) A vertical wall dominated by *Acesta excavata* and *Neopycnodonte zibrowii*, part of an undersampled group of deep-sea habitats. *PLoS ONE*, 8 (11), e79917. <http://dx.doi.org/10.1371/journal.pone.0079917>
- Kenchington, E., Cogswell, A., MacIsaac, K., Beazley, L., Law, B. & Kenchington, T. (2014) Limited depth zonation among bathyal epibenthic megafauna of the Gully submarine canyon, northwest Atlantic. *Deep-Sea Research II*, 104, 67–82. <http://dx.doi.org/10.1016/j.dsr2.2013.08.016>
- Kenchington, E. & Full, W.E. (1994) Fourier analysis of scallop shells (*Placopecten magellanicus*) in determining population structure. *Canadian Journal of Fisheries and Aquatic Sciences*, 51, 348–356. <http://dx.doi.org/10.1139/f94-035>
- Kendall, D.G. (1984) Shape manifolds, Procrustean metrics, and complex projective spaces. *Bulletin of the London Mathematical Society*, 16, 81–121.

<http://dx.doi.org/10.1112/blms/16.2.81>

- Leyva-Valencia, I., Álvarez-Castañeda, S.T., Lluch-Cota, D.B., González-Peláez, S., Pérez-Valencia, S., Vadopalas, B., Ramírez-Pérez, S. & Cruz-Hernández, P. (2012) Shell shape differences between two *Panopea* species and phenotypic variation among *P. globosa* at different sites using two geometric morphometrics approaches. *Malacologia*, 55, 1–13.
<http://dx.doi.org/10.4002/040.055.0101>
- Lima, G.M. & Lutz, R.A. (1990) The relationship of larval shell morphology to mode of development in marine prosobranch gastropods. *Journal of the Marine Biological Association of the United Kingdom*, 70, 611–637.
<http://dx.doi.org/10.1017/S0025315400036626>
- Link, D.H.F. (1807) *Beschreibung der Naturalien-Sammlung der Universität zu Rostock*. 3 Abt. [Part 3], p. 157. Rostock, Adlers Erben.
- Linnaeus, C. (1758) *Systema naturæ per regna tria naturæ, secundum classes, ordines, genera, species, cum characteribus, differentiis, synonymis, locis*. Tomus I. Editio decima, reformata, Laurentii Salvii, Holmiæ [Lipsiæ, Stockholm], pp. [1–4], 1–824.
- López Correa, M., Freiwald, A., Hall-Spencer, J. & Taviani, M. (2005) Distribution and habitats of *Acesta excavata* (Bivalvia: Limidae) with new data on its shell ultrastructure. In: Freiwald, A. & Roberts, J.M. (Eds.), *Cold-water corals and ecosystems*. Springer, Berlin, Heidelberg, pp. 173–205.
- Malchus, N. & Sartori, A.F. (2013) Part N, Revised, Volume 1, Chapter 4 : The early shell: Ontology, features and evolution. *Treatise Online*, 61, 1–144.
- Marshall, B.A. (2001) The genus *Acesta* H. & A. Adams, 1858 in the south-west Pacific (Bivalvia: Limidae). In: Bouchet, P. & Marshall, B.A. (Eds.), *Tropical deep-sea benthos. Publications Scientifiques du Muséum*, 22, pp. 97–109. [Paris]
- McWilliam, H., Li, W., Uludag, M., Squizzato, S., Park, Y.M., Buso, N., Cowley, A.P. & Lopez, R. (2013) Analysis tool web services from the EMBL-EBI. *Nucleic Acids Research*, 41, W597–W600.
<http://dx.doi.org/10.1093/nar/gkt376>
- Ménard de la Groye, F.J.B. (1807) Mémoire sur un nouveau genre de la famille des Solénoïdes. *Annales du Muséum d'Histoire naturelle de Paris*, 9, 131–139.
- Meyer, C.P. (2003) Molecular systematics of cowries (Gastropoda: Cypræidae) and diversification patterns in the tropics. *Biological Journal of the Linnean Society*, 79, 401–459.
<http://dx.doi.org/10.1046/j.1095-8312.2003.00197.x>
- Montagu, G. (1803) *Testacea Britannica or Natural History of British Shells, Marine, Land, and Fresh-water, Including the Most Minute: Systematically Arranged and Embellished with Figures. Vol. 1. & 2.* J. White, London, 606 pp. [xxxvii + 291 pp. & 293–606 pp.]
- Murillo, F.J., Duran Munoz, P., Altuna, A. & Serrano, A. (2011) Distribution of deep-water corals of the Flemish Cap, Flemish Pass and the Grand Banks of Newfoundland (northwest Atlantic Ocean): interaction with fishing activities. *ICES Journal of Marine Science*, 68, 319–332.
<http://dx.doi.org/10.1093/icesjms/fsq071>
- Nei, M. & Kumar, S. (2000) *Molecular Evolution and Phylogenetics*. Oxford University Press, New York, 333 pp.
- Ockelmann, K.W. (1965) Developmental types in marine bivalves and their distribution along the Atlantic coast of Europe. In: Cox, L.R. & Peake, J.F. (Eds.), *Proceedings of the First European Malacological Congress, London, 1962*. Conchological Society of Great Britain and Ireland and the Malacological Society of London, London, pp. 25–35.
- Parr, W.C., Ruto, A., Soligo, C. & Chatterjee, H.J. (2011) Allometric shape vector projection: a new method for the identification of allometric shape characters and trajectories applied to the human astragalus (talus). *Journal of Theoretical Biology*, 272, 64–71.
<http://dx.doi.org/10.1016/j.jtbi.2010.11.030>
- Perez, I., Bernal, V. & Gonzalez, P. (2006) Differences between sliding semilandmark methods in geometric morphometrics, with an application to human craniofacial and dental variation. *Journal of Anatomy*, 208, 769–784.
<http://dx.doi.org/10.1111/j.1469-7580.2006.00576.x>
- Redfearn, P., Chanley, P. & Chanley, M. (1986) Larval shell development of four species of New Zealand mussels: (Bivalvia, Mytilacea). *New Zealand Journal of Marine and Freshwater Research*, 20, 157–172.
<http://dx.doi.org/10.1080/00288330.1986.9516140>
- Rohlf, F.J. (1999) Shape statistics: Procrustes superimpositions and tangent spaces. *Journal of Classification*, 16, 197–223.
<http://dx.doi.org/10.1007/s003579900054>
- Ryan, W.B.F., Carbotte, S.M., Coplan, J.O., O'Hara, S., Melkonian, A., Arko, R., Weissel, R.A., Ferrini, V., Goodwillie, A., Nitsche, F., Bonczkowski, J. & Zemsky, R. (2009) Global Multi-Resolution Topography synthesis. *Geochemistry, Geophysics, Geosystems*, 10, Q03014.
<http://dx.doi.org/10.1029/2008GC002332>
- Sheets, H.D. (2001) *IMP: PCAGen6- Principal Components Generation Utility*. Department of Physics, Canisius College, Buffalo, NY. Available from: <http://www3.canisius.edu/~sheets/morphsoft.html> (accessed 23 June 2015)
- Sheets, H.D. (2002) *Imp: SemiLand6*. Department of Physics, Canisius College, Buffalo, NY. Available from: <http://www3.canisius.edu/~sheets/morphsoft.html> (accessed 23 June 2015)
- Sheets, H.D. (2003) *IMP: CoordGen6-Coordinate Generation Utility: User's Manual*. Department of Physics, Canisius College, Buffalo, NY. Available from: <http://www3.canisius.edu/~sheets/morphsoft.html> (accessed 23 June 2015)

- Sheets, H.D. (2004) *IMP - Integrated Morphometrics Package*. Department of Physics, Canisius College, Buffalo, NY. Available from: <http://www3.canisius.edu/~sheets/morphsoft.html> (accessed 23 June 2015)
- Sheets, H.D. (2006) *CVAGen version 6*. Department of Physics, Canisius College, Buffalo, NY. Available from: <http://www3.canisius.edu/~sheets/moremorph.html> (accessed 23 June 2015)
- Sheets, H.D., Covino, K.M., Panasiewicz, J.M. & Morris, S.R. (2006) Comparison of geometric morphometric outline methods in the discrimination of age related differences in feather shape. *Frontiers in Zoology*, 3, 15. <http://dx.doi.org/10.1186/1742-9994-3-15>
- Sneli, J.-A., Knudsen, J. & Vedelsby, A. (2009) Johan Christian Fabricius and his molluscan species, *Acesta excavata* (J. C. Fabricius, 1779). *Steenstrupia*, 30, 153–162. Available from: http://zoologi.snm.ku.dk/english/about_the_zoological_museum/publications/steenstrupia/early_volumes/Sneli_et_al_2009.pdf (accessed 10 August 2015)
- Sowerby, G.B.I. (1823) *The genera of Recent and fossil shells, for the use of students in conchology and geology*. Vol. 1. London, pl. 113, fig. 4.
- Sowerby, G.B. III. (1883) Descriptions of five new species of shells. *Proceedings of the Zoological Society of London*, 1883, 30–32.
- Sowerby, G.B. III. (1888) Descriptions of sixteen new species of shells. *Proceedings of the Zoological Society of London*, 1888, 207–213.
- Tamura, K. & Nei, M. (1993) Estimation of the number of nucleotide substitutions in the control region of mitochondrial DNA in humans and chimpanzees. *Molecular Biology and Evolution*, 10, 512–526. Available from: <http://mbe.oxfordjournals.org/content/10/3/512> (accessed 10 August 2015)
- Tamura, K., Nei, M. & Kumar, S. (2004) Prospects for inferring very large phylogenies by using the neighbor-joining method. *Proceedings of the National Academy of Sciences*, 101, 11030–11035. <http://dx.doi.org/10.1073/pnas.0404206101>
- Tamura, K., Stecher, G., Peterson, D., Filipinski, A. & Kumar, S. (2013) MEGA6: Molecular Evolutionary Genetics Analysis version 6.0. *Molecular Biology and Evolution*, 30, 2725–2729. <http://dx.doi.org/10.1093/molbev/mst197>
- Tautz, D., Arctander, P., Minelli, A., Thomas, R.H. & Vogler, A.P. (2003) A plea for DNA taxonomy. *Trends in Ecology and Evolution*, 18, 70–74. [http://dx.doi.org/10.1016/S0169-5347\(02\)00041-1](http://dx.doi.org/10.1016/S0169-5347(02)00041-1)
- Vokes, H.E. (1963) Studies on Tertiary and Recent giant Limidae. *Tulane Studies in Geology*, 1, 73–92.
- Webster, M. & Sheets, H.D. (2010) A Practical introduction to landmark-based geometric morphometrics. In: Alroy, J. & Hunt, G. (Eds), *Quantitative methods in Paleobiology*. Paleontological Society Papers, 16, 163–188, plus Supplementary Online Material, 43 pp. Available from: http://www.paleosoc.org/shortcourse2010/webster_and_Sheets2010SOM.pdf (accessed 23 June 2015)
- Zelditch, M.L., Swiderski, D.L. & Sheets, H.D. (2012) *Geometric morphometrics for biologists: a primer*. 2nd Edition. Elsevier Academic Press, London, 478 pp.